RD&E

CENTER

Technical Report

No. 13293

DURABILITY TESTING OF

TANK TRACK RUBBER COMPOUNDS

UNDER CYCLIC LOADING

MIPR NUMBER W56HZW-85-EKE-02

October 1987

By Gregory B. McKenna & Kathleen M. Flynn
Polymers Division
National Bureau of Standards
Gaithersburg, Maryland 20899

Approved for Public Release:
Distribution Unlimited

U.S. ARMY TANK-AUTOMOTIVE COMMAND
RESEARCH, DEVELOPMENT & ENGINEERING CENTER
Warren, Michigan 48397-5000

UNCLASSIFIED

SECURITY CLASSIFICATION OF THIS PAGE

REPORT DOCUMENTATION PAGE

Form Approved
OMB No 0704-0188
Exp. Date Jun 30, 1986

1a. REPORT SECURITY CLASSIFICATION Unclassified	1b. RESTRICTIVE MARKINGS
2a. SECURITY CLASSIFICATION AUTHORITY	3. DISTRIBUTION/AVAILABILITY OF REPORT Unlimited
2b. DECLASSIFICATION/DOWNGRADING SCHEDULE	
4. PERFORMING ORGANIZATION REPORT NUMBER(S)	5. MONITORING ORGANIZATION REPORT NUMBER(S) 13293
6a. NAME OF PERFORMING ORGANIZATION National Bureau of Standards 6b. OFFICE SYMBOL (If applicable)	7a. NAME OF MONITORING ORGANIZATION U.S. Army Tank-Automotive Command
6c. ADDRESS (City, State, and ZIP Code) Gaithersburg, MD 20899	7b. ADDRESS (City, State, and ZIP Code) Warren, MI 48397-5000
8a. NAME OF FUNDING/SPONSORING ORGANIZATION 8b. OFFICE SYMBOL (If applicable)	9. PROCUREMENT INSTRUMENT IDENTIFICATION NUMBER MIPR No. W46HZW-85-EKE-02
8c. ADDRESS (City, State, and ZIP Code)	10. SOURCE OF FUNDING NUMBERS PROGRAM ELEMENT NO. / PROJECT NO. / TASK NO. / WORK UNIT ACCESSION NO

11. TITLE (Include Security Classification)
Durability Testing of Tank Track Rubber Compounds under Cyclic Loa g (u)

12. PERSONAL AUTHOR(S)
McKenna, Gregory B. and Flynn, Kathleen M.

13a. TYPE OF REPORT	13b. TIME COVERED	14. DATE OF REPORT (Year, Month, Day)	15. PAGE COUNT
Annual	FROM 10/1/85 TO 9/30/86	October 15, 1987	55

16. SUPPLEMENTARY NOTATION

17. COSATI CODES		
FIELD	GROUP	SUB-GROUP

18. SUBJECT TERMS (Continue on reverse if necessary and identify by block number)
Cycle Shifted Failure Envelope; Durability Testing, Failure Modeling; Rubber Compounds; Tank Track Pads, tanks (combat vehicles)

19. ABSTRACT (Continue on reverse if necessary and identify by block number)

The mechanical durability of three tank track rubber compounds, designated as 15TP-14AX 15NAT-25A and 15TP-R were evaluated within the framework of a cycle shifted failure envelope (CSFE) model for rupture of carbon black filled rubbers. It was found that, while the CSFE model is imperfect, it serves as a useful framework for evaluating the mechanical durability of the rubber compounds. The three rubber compounds could be ranked for durability in creep and in zero tensile sinusoidal fatigue. The results show that the ranking varies with test conditions, e.g., temperature, test frequency, etc. New results are presented showing violation of the classical failure envelope model.

(Keywords: ———)

20. DISTRIBUTION/AVAILABILITY OF ABSTRACT ☐ UNCLASSIFIED/UNLIMITED ☒ SAME AS RPT. ☐ DTIC USERS	21 ABSTRACT SECURITY CLASSIFICATION Unclassified
22a. NAME OF RESPONSIBLE INDIVIDUAL Jacob Patt	22b TELEPHONE (Include Area Code) (313) 574-8687 22c. OFFICE SYMBOL

DD FORM 1473, 84 MAR 83 APR edition may be used until exhausted
All other editions are obsolete.

SECURITY CLASSIFICATION OF THIS PAGE
UNCLASSIFIED

TABLE OF CONTENTS

LIST OF TABLES

LIST OF ILLUSTRATIONS

1.0. INTRODUCTION

This is the second annual report for the program "Durability Testing of Tank Track Rubber Compounds Under Cyclic Loading," MIPR Number W56HZW-85-EKE-02. In this report we describe work carried out between October 1, 1985 and September 30, 1986.

The purpose of the research being performed here is to develop a testing methodology for evaluation of the mechanical durability of carbon-black-filled rubbers used in track pads on U.S. Army tracked vehicles. The original scope of this work was to characterize three track pad rubbers within the framework of a cycle shifted failure envelope (CSFE) model which had proven successful in describing the failure behavior of a carbon-black-filled butyl rubber[1,2] . A tri-blend designated 15TP-14AX, a natural rubber compound designated 15NAT-25A and a commercial rubber of unknown composition designated 15TP-R were selected for evaluation and to validate the CSFE model for these highly loaded elastomers. In the first annual report[1], work was described from which it was preliminarily concluded that, for the 15TP-14AX rubber the CSFE model was useful as a predictor of lifetime, but with the stipulation that the failure envelope of interest be the creep failure envelope rather than that obtained from constant rate of stretching experiments. At that time, adequate data had not been obtained to evaluate the model validity for the 15NAT-25A or the 15TP-R rubbers.

As will be discussed, the more extensive results from the current work show that a simple CSFE failure model is not valid for any of the rubber compounds investigated here, but it is a useful framework for materials evaluation and provides an important means for characterizing the durability of the rubbers under consideration.

Finally, we note that the work strongly suggests that other rubber compounds which can better withstand the high temperatures (~150 °C) seen by the tank track pads be evaluated. A proposal is made to test three such compounds using the same methodology described in the subsequent sections.

2.0. SUMMARY

During the reporting period, 1 October 1985 - 30 September 1986, work was continued to evaluate the mechanical durability of three rubber compounds used or under consideration for use in tank track pad applications. The approach taken used the CSFE model as a framework within which to evaluate the materials. The first conclusion we can make from the work carried out during this reporting period is that the CSFE model is not applicable to any of the rubber compounds studied. The reason for this and a surprising result is that the failure envelopes for these rubbers depend upon the type of testing even in quasi-static tests (i.e., creep or constant rate of elongation),

contrary to literature reports for many other rubber systems[17]. Furthermore, the failure envelopes in creep or in fatigue loading obtained at room temperature differ from those obtained at T ≥ 75 °C.

The CSFE model, however, is still a useful framework for carrying out durability tests on rubber compounds. In particular, the creep and fatigue failure data obtained allow the evaluation of the durability of the three rubber compounds. There are four additional conclusions which we can make from the data obtained thus far in this study:

- In creep loading at 23 °C and at high stresses, (≥10 (MPa)) the 15NAT-25A rubber compound shows the greatest resistance to failure, i.e., $t_{f_{15NAT-25A}} > t_{f_{15TP-14AX}} \approx t_{f_{15TP-R}}$. All three rubber compounds have similar failure times for 6 MPa < σ< 10 MPa. Below 6 MPa the 15TP-14AX shows the longest lifetime.

- As the temperature increases, the relative creep rupture resistance of the rubber compounds changes from that at 23 °C. Thus, at 175 °C the lifetimes order as $t_{f_{15TP-14AX}} > t_{f_{15TP-R}} > t_{f_{15NAT-25A}}$.

- The lifetime of the 15TP-14AX and 15NAT-25A rubbers under zero tension sinusoidal fatigue loading at 23 °C can be described by an equation of the $t_f = A\omega^{\gamma}\sigma_p^{\beta}$ where t_f is the time to failure, ω is the test frequency and σ_p is the peak stress. The fact that $|\gamma|$ is less than 1 for both rubbers means that the common practice of increasing test frequency as a means of test acceleration can result in overprediction of the material lifetime at lower frequencies. The scatter in the data for the 15TP-R rubber compound precludes application of the equation unless more data were t. be obtained.

- The relative resistance to fatigue of the three rubber compounds depends upon the stress level and the test frequency. The 15TP-14AX rubber shows the greatest stress sensitivity while the 15NAT-25A shows the greatest frequency sensitivity of the respective times-to-failure. At the lowest frequency (0.0002 Hz) the fatigue lifetimes order as $t_{f_{15TP-14AX}} > t_{f_{15NAT-25A}} \approx t_{f_{15TP-R}}$. At the highest test frequency they order as $t_{f_{15TP-14AX}} \approx t_{f_{15TP-R}} > t_{f_{15NAT-25A}}$

Finally, a brief description of proposed future work to address the problem of high-temperature resistant, but conventional rubbers, is presented.

3.0. DISCUSSION

3.1. Background

3.1.1. Stress Softening and Damage Accumulation in Filled Rubbers. The phenomenon of stress softening is known to occur in both filled and some

unfilled elastomers[3-8]. Of particular interest is the work of Derham and Thomas[9] in which they reported on the creep behavior of a carbon-black-reinforced natural rubber subjected to load-unload cycling. They found that the creep rate was greater under cyclic loading than under static loading and that the rate of cyclic creep followed a logarithmic law (with cycle number) and did not tend towards a constant value. Figure 3-1 depicts their findings showing the "accelerated" creep due to cyclic loading.

In studying the failure behavior of filled rubber, McKenna and Penn[10] found that lifetime under load-unload cycling depends upon both frequency and waveform and that the dependence could not be described by either a time-dependent, cumulative damage approach (for which lifetime would be independent of test frequency) or a cycle-dependent, cumulative damage approach (for which the total number of cycles to failure would be constant independent of test frequency and waveform). As shown in Figure 3-2, lifetime for a carbon-black-filled polyolefin rubber was found to be much shorter than either the creep failure time or that expected from a cumulative damage prediction--thus, failure was "accelerated" due to the cyclic loading.

The CSFE failure model was developed in order to establish a link between the observed "accelerated" creep and the "accelerated" failure behaviors of carbon-black-filled rubber. The link was made through a failure envelope similar to that originally proposed by T.L. Smith[11-17]. Details are presented in the next section.

3.1.2. The Failure Model. Some years ago, Smith[11-15] proposed the concept of a failure envelope for which the locus of stress-at-break (σ_b) vs. strain-at-break (ϵ_b) for a rubber can be represented as a unique curve independent of deformation or stress history. Figure 3-3 shows a typical failure envelope. (Note that the failure stress is reduced by the temperature to account for the modulus variation with temperature.) This is a reasonable approximation for simple deformation histories such as constant rate of deformation, stress relaxation or creep. However, in the presence of a stress-softening effect, Smith found that the failure envelope could shift to larger strains[14,15].

In our previous work[2], we were able to use creep data taken under cyclic loading conditions combined with the notion of a shifted failure envelope to account for the frequency and waveform dependencies of the fatigue lifetimes of a carbon-black-filled butyl rubber. The shifted failure envelope is represented by a simple equation which relates the failure envelope in simple deformation histories to that in cyclic histories. For the strain-at-break we found[2]:

$$\epsilon_{bc} = \alpha_\sigma \epsilon_{bo} \qquad (1)$$

where ϵ_{bc} is the strain-at-break under cyclic load, α_σ is a shift factor (which may depend on the stress level, frequency, etc.) and ϵ_{bo} is the failure strain (at the same stress) in a simple deformation history. Then, if it is assumed that α_σ is a constant independent of stress,

frequency, etc., then fatigue lifetime can be predicted simply by extrapolation of the cyclic creep curve to the ϵ_{bc} determined by equation (1) and a single set of failure data. For the filled butyl rubber $\alpha_\sigma = 1.67$ was determined from failure data obtained at 0.09 Hz. Figure 3-4 shows a comparison of the lifetime predicted from the model and the lifetimes obtained experimentally. As can be seen the agreement is reasonable. We note that the extrapolations were made from short time creep data obtained for $0.1N_f \leq N \leq 0.33\ N_f$ depending upon the test frequency and waveform. We will refer to the cycle shifted failure envelope model of failure by the acronym CSFE.

3.1.3. Summary of First Year's Work. During the first year work was accomplished in the evaluation of three rubber compounds within the framework of a CSFE model for failure of filled rubbers. The failure envelopes for all three elastomers, designated as 15TP-14AX, 15NAT-25A and 15TP-R, were obtained under constant rate of deformation conditions and are depicted in Figure 3-5. As can be seen, the 15TP-14AX and 15TP-R systems have constant rate failure envelopes which are similar, although the 15TP-14AX rubber fails at somewhat smaller strains (for the same stress) at the low-stress (high-temperature) end of the failure envelope. The 15NAT-25A rubber has a constant rate failure envelope which is shifted to the right (to larger strains) by a factor of 3 to 5 relative to the envelopes which characterize the other two rubbers.

The CSFE model requires the characterization of the creep and cyclic loading behavior of the rubber. During the first year, we essentially completed the evaluation of the creep and cyclic loading response of the 15TP-14AX rubber under ambient conditions. There were four principal findings:

- The cyclic creep rate for the 15TP-14AX rubber ($d\log(\epsilon)/d\log(N-1)$) is greater than that obtained under constant loading conditions ($d\log(\epsilon)/d\log(t)$). However, the amount of acceleration due to the cyclic loading is not as great as had been observed previously with a filled butyl rubber[2].

- The failure envelope which characterizes the creep rupture of the 15TP-14AX rubber does not fall on the failure envelope which characterizes the breaking of the rubber in constant rate of deformation tests. This is shown in Figure 3-6. To our knowledge, this is the first time that such anomalous behavior has been reported. It is possible that the rubber during the creep tests, which last longer than do the constant rate of deformation tests, is attacked by ozone or that strain crystallization occurs.

- For the 15TP-14AX rubber the failure envelope obtained in zero-tension sinusoidal loading appears to be shifted superposably relative to the creep failure envelope rather than the constant rate failure envelope. This was interpreted to imply that the CSFE model, in order to be generally applied, need only consider a shift relative to the failure envelope in creep loading rather than

relative to the constant rate failure envelope. If both failure envelopes coincide, of course, this distinction is obviated.

- The lifetimes of the 15TP-14AX rubber under creep loading and sinusoidal loading conditions were significantly different. The fatigue loading "accelerated" failure by up to two orders of magnitude relative to the lifetime obtained under creep rupture conditions. The amount of failure "acceleration" depended upon the testing frequency, lifetime at low frequencies being longer than at high frequencies. This can be seen by comparing Figure 3-7, which shows the time-to-failure versus applied stress under creep conditions, with Figure 3-8, which depicts fatigue lifetime versus peak stress for various test frequencies.

Because the behavior of the 15TP-14AX rubber appeared to be describable using the CSFE model point above, the First Annual Report[1] ended with a note of optimism that the model is suitable for carrying out accelerated testing in the evaluation of carbon-black-filled rubber. As we will see in the sections which follow, some of this optimism must be replaced by caution.

3.2. Method of Experimentation

3.2.1. Materials. There have been three rubber compounds studied during the past year. All were carbon-black-filled compounds which were provided to us by P. Touchet of the U.S. Army Belvoir Research and Development Center. These compounds were received in the form of 152 mm by 152 mm by 2 mm sheets (6" by 6" by 0.08"). The butyl rubber compound described in the prior study[4] was made in the laboratories of the National Bureau of Standards in the form of 152 mm by 152 mm by 1 mm sheets. The rubber formulations are given in Table 3-1.

3.2.2. Mechanical Properties Testing. Mechanical properties testing was performed on non-standard-size dumbbell samples in order that fatigue testing results could be compared with the results from creep and constant rate of deformation experiments. The nonstandard dumbbell specimens had a width in the gauge section of 6.4 mm (0.25 inch) a gauge length of 25 mm (1.0 inch) a maximum width in the grips of 13 mm (0.5 in) and an overall length of 75 mm (3.0 in).

Creep data were obtained at room temperature (23 $\pm$ 1 °C) by hanging weights from the samples and measuring the separation of two gauge marks using a cathetometer. Time-to-rupture was recorded for each sample. Creep data at elevated temperature were obtained in the same manner as at room temperature with the addition of a specially designed temperature chamber which allowed simultaneous testing of six samples. Test temperatures were 75, 125 and 175 °C $\pm$ 1 °C.

Fatigue data were obtained at room temperature (23 $\pm$ 1 °C) using a servohydraulic testing machine with a total stroke capacity of 152 mm (6 in). The strain measurements under cyclic loading were obtained by measuring the separation of gauge marks using a steel rule of graduated

each 2.5 mm. The original gauge separation was 12.7 mm. Results are reported at the maximum load in the cycle. Tests were carried out in zero-tension sinusoidal loading at frequencies from 2 by 10^{-4} to 5 by 10^{-2} Hz. This range of testing frequency was chosen to assure that the tests were isothermal and that hysteretic heating did not occur. The number of cycles to failure was obtained for each sample. Elevated temperature fatigue test results were obtained using a standard oven on the hydraulic test machine fatigue tests were performed at 75, 125 and 175 $\pm$ 1 °C.

3.3. Results

3.3.1. 15TP-14AX Rubber Compound. Much of the testing carried out on the 15TP-14AX rubber compound was a continuation of work begun during the first year of the contract. In particular creep and fatigue testing at room temperature were continued to complete these aspects of the characterization of the 15TP-14AX. In addition, new work was initiated during this reporting period to characterize the creep failure and fatigue failure behavior of the 15TP-14AX rubber at elevated temperatures. These are discussed below.

3.3.1.1. 15TP-14AX: Failure behavior under creep loading conditions. Characterization of the creep failure behavior of the 15TP-14AX rubber was carried out at 23, 75, 125 and 175 °C. The logarithm of the time to failure vs. the applied (engineering) stress is shown in Figure 3-9. The data at elevated temperatures are insufficient to establish whether or not the stress dependence of the failure time is the same as at 23 °C. However, as depicted by the dashed lines, such a possibility is definitely within the experimental scatter of the data. Assuming this to be the case, then the temperature dependence of the failure time can be obtained. As shown in Figure 3-10, there is a change in the temperature dependence at T $\approx$ 75 °C, where there is an increase in the temperature sensitivity corresponding to an increase in activation energy. Interestingly, this is at approximately the melting point of the waxy hydrocarbon blend used in the compound formulation for the 15TP-14AX (see Table 3-1). It is unknown whether there is a correlation between the presence of the waxy hydrocarbons and the change in activation energy.

This apparent change in behavior at approximately 75 °C is reflected in the failure envelope obtained from the elevated temperature measurements. As seen in Figure 3-11, the data obtained at 75, 125, and 175 °C fall on approximately the same curve, which is significantly different from that obtained at 23 °C. Here we recall that we had previously found[1] that the creep failure envelope for the 15TP-14AX differs significantly from that obtained from constant rate of elongation experiments. It now appears that the creep envelope itself may show different regimes, depending upon the temperature of test. We remark further that the creep failure envelope at the higher temperatures does not coincide with the failure envelope obtained in constant rate of deformation tests. The three failure envelopes are depicted in Figure 3-12.

3.3.1.2. 15TP-14AX: Fatigue failure behavior. The part of the program to characterize the fatigue failure behavior of the 15TP-14AX rubber at ambient temperatures has been virtually completed. The results are best summarized by examining Figures 3-13 and 3-14 where we show in double logarithmic representations the time-to-failure versus peak load and test frequency, respectively. As can be seen, the failure times under cyclic loading decrease dramatically as load or frequency increase over the range of parameters studied. The fatigue lifetime at ambient conditions is adequately described by an equation of the form

$$t_f = A\,\omega^{\gamma}\sigma^{\beta} \qquad (2)$$

where A, γ and β are constants whose values obtained from a least squares regression are tabulated in Table 3-2, ω is the test frequency in Hz and σ is the peak stress. Interestingly, t_f shows a power law dependence on both frequency and stress. Furthermore, the fact that $|\gamma| < 1$ shows that a common practice of increasing testing frequency to "accelerate" the fatigue test has the effect here of overestimating the lifetime at lower test frequencies. A comparison of the fatigue lifetimes with those obtained in creep shows them to be nearly two orders of magnitude shorter at the higher test frequencies, as observed previously for carbon-black-filled rubber[2,10].

Several fatigue tests were also run at elevated temperatures. The results are depicted in Figure 3-15, along with the lines from equation (2) for the data obtained at 23 °C. Because the stress dependence is approximately the same for the elevated temperature tests as for those at 23 °C, we have chosen to assume that the temperature dependence can be obtained by taking a cross plot of the data at 6.2 MPa. Then, as shown in Figure 3-16, the apparent activation energy shows a change at T≈75 °C, as was the case for the creep failure. Interestingly, the apparent activation energies for fatigue failure and creep failure are approximately the same. Difficulties in carrying out strain measurements at elevated temperatures limited the amount of data obtained for construction of the failure envelope in fatigue. Results for 23 °C and 75 °C are depicted in Figure 3-17. Although there is significant scatter in the results, the data point at 75 °C (triangle) in Figure 3-17 is apparently outside the range of the experimental scatter and indicates that, as was the case in the creep experiments, the higher temperature failure envelope is different from that obtained at 23 °C.

Finally, in Figure 3-18 we compare the constant rate of deformation failure envelope with those obtained in creep and from fatigue. These results demonstrate that, unlike results reported in the literature for many rubber compounds,[11-15,17] there is no simple description of the failure behavior of the 15TP-14AX in terms of a failure envelope.

Future work requires a more complete characterization of the stress, temperature, frequency and waveform dependencies of the fatigue behavior of the 15TP-14AX rubber.

3.3.2. 15NAT-25A Rubber Compound. The failure behavior of the 15NAT-25A rubber compound at room temperature and at elevated temperatures has been partially characterized. A considerable amount of effort was put into attempting to determine the fatigue characteristics of this rubber, but two major problems, which were only overcome towards the end of this reporting period, contributed to a slowdown in the characterization of this material. First, the servohydraulic machine has only 6 inches of stroke and the high extensibility of the 15NAT-25A rubber often led to saturation of the stroke capacity of the machine prior to failure. This problem was solved by shortening the samples. Second, there has been considerable difficulty with samples failing in or slipping out of the grips prior to failure in the gauge section. This problem has not been completely eliminated, but has been ameliorated by changing the grip geometry and the facing material on the grip surfaces. Below we report the results of creep to failure and fatigue testing for the 15NAT-25A rubber compound.

3.3.2.1. 15NAT-25A: Failure behavior under creep loading conditions. Failure times of the 15NAT-25A rubber compound under constant load at 23, 75, 125 and 175 °C are depicted in Figure 3-19. Although there is significant scatter in these data, it is obvious that the behavior is different from that obtained for the 15TP-14AX. Apart from the magnitude of the failure times at a given stress, to be discussed subsequently, the data at different temperatures for the 15NAT-25A do not show the same stress dependence, as did the 15TP-14AX. Therefore, a simple expression of the temperature and stress dependence of the lifetime:

$$t_f = F(T) \bullet H(\sigma) \qquad (3)$$

which could represent the data for the 15TP-14AX cannot represent the data for the 15NAT-25A. Therefore, we have not depicted the temperature dependence of the lifetime for this rubber.

The failure envelope for the 15NAT-25A rubber under creep conditions depends upon temperature as did that of the 15TP-14AX rubber. This is depicted in Figure 3-20, where we see that above 75 °C, the failure points lie on a different curve than those obtained at 23 °C. Interestingly, the part of the creep failure envelope obtained thus far at high temperatures in creep is not, greatly different from that obtained from the constant rate of deformation experiments. This can be seen in Figure 3-21.

3.3.2.2. 15NAT-25A: Fatigue failure behavior. As mentioned above fatigue failure data were difficult to obtain on the 15NAT-25A rubber compound. The results obtained for time-to-failure vs applied stress at several different frequencies are depicted in Figure 3-22. A plot of lifetime vs. frequency at different stress levels is shown in Figure 3-23. Within the experimental uncertainty the results can be represented by equation 2. The parameters required for the fit are shown in Table 3-2 and the fact that $|\gamma| < 1$ implies, as discussed

previously for the 15TP-14AX rubber, that increasing testing frequency as a means of accelerating the fatigue testing process can lead to overestimates of lifetime at lower frequency. (See McKenna and Penn for a discussion of this.)

A comparison of the fatigue lifetimes in Figure 3-22 with the creep lifetimes shown in Figure 3-19 reveals that the cycling process "accelerates" failure in this rubber, i.e., fatigue lifetimes are a decade or more shorter than in static loading. This is expected from strain crystallization and melting upon cycling in natural rubber compounds.[9]

Finally, no elevated temperature fatigue tests were carried out for the 15NAT-25A rubber and insufficient data were obtained to construct the cyclic failure envelope for this rubber. These are tasks which should be undertaken in the future.

3.3.3. 15TP-R Rubber Compound. The creep and fatigue failure behaviors of the 15TP-R rubber compound at ambient temperatures have been extensively characterized. However, as discussed below, the large amount of scatter in the failure times under both static and dynamic loading conditions makes additional testing necessary to complete the characterization of the failure behavior of this rubber at room temperature (23 °C). Additional work was also begun to determine the failure behavior of this rubber compound under creep and fatigue loading conditions at elevated temperatures. These results are described below.

3.3.3.1. 15TP-R: Failure behavior under creep loading conditions. The failure behavior of the 15TP-R rubber compound under constant load (creep) conditions at 23, 75, 125 and 175 °C is shown in Figure 3-24 as a plot of the logarithm of the failure time versus the applied stress. As can be seen there is significant scatter in the data. Within the limits of the data, it appears that the stress dependence of lifetime varies with temperature. Further work would be required to determine whether or not this is true.

Reduction of the creep failure data to construct a failure envelope shows that, as with the 15TP-14AX and 15NAT-25A rubber compounds, the 15TP-R compound appears to have a failure envelope for high temperatures which differs from that obtained at 23 °C. This is depicted in Figure 3-25. As with the other two rubber compounds, the failure envelope obtained at $T \geq 75$ °C is shifted to higher strains at failure. Also of interest is the observation that the scatter in the failure times observed in experiments carried out at 23 °C is not reproduced in the failure envelope.

Finally, as shown in Figure 3-26, neither the low temperature nor the high-temperature creep failure envelope coincides with that obtained from constant rate of deformation experiments.

3.3.3.2. 15TP-R: Fatigue failure behavior. The fatigue failure behavior of the 15TP-R rubber compound at 23 °C is depicted in Figure

3-27 as a plot of the logarithm of time-to-failure versus the peak stress. The different test frequencies are denoted by the different symbols in the figure caption and the lines are drawn to show an approximate behavior at 0.0002, 0.01 and 0.05 Hz. As can be seen from the figure, there is an enormous amount of variability in the failure lifetime of this rubber. However, the trends are as with the other two rubber compounds described previously, i.e., lifetime decreases as stress and frequency increase. For the 15TP-R rubber, however, the large amount of variability in the data results in the need for more testing a quantitative assessment of these dependencies to be carried out. Importantly, the fatigue lifetime at 23 °C is lower than the creep lifetime by a decade or more (compare Figure 3-27 with Figure 3-24).

As was the case for the creep behavior for this rubber, the failure envelope in fatigue exhibits less variability than the failure times themselves. This is shown in Figure 3-28. In Figure 3-29 we see that the fatigue failure envelope intersects the one determined from constant rate of deformation experiments and differs from the two (high- and low-temperature) failure envelopes obtained in creep.

3.4. Comparison of the Durability of the 15TP-14AX, 15NAT-25A and 15TP-R Rubber Compounds

A major feature of the work here has been the characterization of the mechanical durability of three different rubber compounds using the same testing methodology. At this point in the study, the data so far accumulated can be used to provide a comparison of the lifetimes of the rubbers subjected to two different types of loading--creep and zero-tension sinusoidal fatigue. In the discussion which follows we compare the failure behaviors of the 15TP-14AX, 15NAT-25A and 15TP-R rubber compounds described individually in the previous paragraphs.

The resistance to failure under creep loading is best compared by simply plotting the lifetimes versus applied stress for the three rubbers. This is done in figure 3-30 for 23, 75, 125 and 175 °C, where the curves traced in the relevant figures presented previously are shown without the data points. We can make several points from examination of Figure 3-30--keeping in mind that at higher temperatures the data represented by the curves are sparse. First, the relative resistance to creep failure of the three rubber compounds depends upon the stress level of interest as well as the temperature. Thus at 23 °C, above approximately 10 MPa of stress, the 15NAT-25A compound is clearly superior to the other two rubber compounds which show similar behaviors above 10 MPa. Between 6 and 10 MPa the three rubbers show similar lifetimes, i.e., resistances to failure. However; below approximately 6 MPa the curve for the 15TP-14AX rubber begins to turn upwards, suggesting that this rubber may be superior at low stress levels.

Similarly, at 25 and 125 °C the 15NAT-25A rubber takes longer to fail than the other two above approximately 4 MPa, while the 15TP-14AX appears superior at lower stresses. At 175 °C, the ordering is such

that the 15TP-14AX lasts longer than does the 15TP-R which lasts longer than the 15NAT-25A.

Thus, in creep loading conditions at high stresses and below 125 °C, the 15NAT-25A appears superior to the other two rubbers. However, at low stress the 15TP-14AX appears to resist failure better than either the 15NAT-25A or 15TP-R compounds.

In Figure 3-31 we show a comparison of the fatigue lifetime vs. peak stress for the three rubber compounds at 0.0002 Hz and 0.05 Hz. At the lower frequency, the 15TP-14AX definitely shows a greater resistance to fatigue failure than either the 15NAT-25A or the 15TP-R rubbers, while the 15TP-R and the 15NAT-25A rubbers show similar behaviors. At 0.05 Hz, the 15NAT-25A rubber definitely shows poorer performance than the other two compounds. A true comparison of the 15TP-14AX rubber and the 15TP-R rubber at the higher frequency (0.05 Hz) is difficult due to the large amount of scatter in the data for the 15TP-R rubber (recall Figure 3-27). However, based upon the traces shown in Figure 3-31, one would conclude that the 15TP-14AX will perform better at low peak stresses (σ_p < 10 MPa) while the 15TP-R will perform better above this value of σ_p.

The important point to be made here is that the relative fatigue resistances of the rubbers depends upon test frequency and the peak stress level. Thus, under low stress and low frequencies, the 15TP-14AX rubber out- performs the other two by an order of magnitude or more. On the other hand, while the 15NAT-25A rubber and 15TP-R rubber show similar fatigue resistances at low frequencies, at high testing frequency the 15NAT-25A has a lifetime approximately one order of magnitude lower than that of either the 15TP-R or the 15TP-14AX.

3.5. Proposed Future Work

3.5.1. Continued Characterization of 15TP-14AX and 15NAT-25A Rubber Compounds. The first point to be made here is that in conjunction with Mr. Jacob Patt of the U.S. Army Tank-Automotive Command, Research and Development Center, Warren, Michigan, we have decided to discontinue testing of the 15TP-R rubber compound. This is a reasonable decision for two reasons. First the compound is a commercial one of unknown formulation. Second, the variability in the data from this compound is much greater than for the other two and would force a significantly greater and unwarranted number of tests to adequately characterize the failure behavior of this material.

Future work to characterize the 15TP-14AX and 15NAT-25 rubber compounds should continue in order to complete the fatigue characterization of the 15NAT-25 at 23°C. The elevated temperature behavior in creep and fatigue of both rubber compounds should also be more thoroughly examined in order to establish the temperature sensitivities of the creep and fatigue processes in these materials. Also new testing should be undertaken to examine the effects of waveform on the lifetime of these two rubber compounds. Sinusoidal and square wave tests with only

partial unloading should be performed as it is known that such variations in loading conditions can greatly affect fatigue lifetime[2].

3.5.2. Characterization of Higher Temperature Rubber Compounds. Temperatures in rubber tank track pads during maneuvers or combat have been estimated to reach in excess of 150 °C[18] which can result in significant reductions in the durability of conventional elastomers, as observed earlier in this report. In order to evaluate the importance of temperature on the mechanical durability question for tank track pad elastomer, we propose to examine the response at elevated temperatures of several "conventional" rubber compounds. As was seen in the previous sections of this report, elevated temperatures can reduce lifetime by several orders of magnitude. Furthermore, the relative performance of the compounds changes when the temperature increases from ambient. Therefore, we feel that a useful expansion of the work carried out to date on this contract would be the addition of several rubber compounds which are generally more temperature resistant, but not normally considered as having as much ambient temperature mechanical durability as the isoprene or butadiene based elastomers considered so far.

To this effect three compounds have been chosen for preliminary study. They were chosen from among several thousand recipes which have been collected over the years at the National Bureau of Standards and include a nitrile rubber compound and two different EPDM-type rubber compounds. The proposed formulations are shown in Tables 3-3 and 3-4. These compounds may not be optimal but were selected with the purpose of obtaining compounds having higher temperature resistance than those currently being evaluated and to have reasonable ASTM-type mechanical properties. This will, in principle, allow the demonstration of improved high temperature performance of the rubber compounds in spite of relatively unimpressive ambient temperature properties.

These compounds will be made in our laboratories. We propose to make a sufficient quantity so that should TACOM be interested there will be enough material to pass along to other groups for evaluation. The characterization of these materials will follow the same route as for the original three rubber compounds, i.e., they will be characterized within the framework of the CSFE model for rupture of rubber. However, due to inadequacies of the CSFE model described in this report, work will also be commenced to examine or develop other models of rupture to describe/predict the data.

LIST OF REFERENCES

[1] G.B. McKenna, "Durability Testing of Tank Track Rubber Compounds Under Cyclic Loading", First Annual Report, U.S. Army Tank Automotive Command R and D Center Laboratory Technical Report No. 13148, May 1986.

[2] G.B. McKenna and L.J. Zapas, Rubber Chem. Technol., 54, 718 (1981).

[3] L. Mullins, Rubber Chem. Technol., 42, 339 (1969).

[4] J.B. Donnet and A. Voet, "Carbon Black: Physics, Chemistry, and Elastomer Reinforcement", Marcel Dekker, Inc. New York (1976).

[5] E.M. Dannenberg and J.J. Brennan, Rubber Chem. Technol., 39, 597 (1966)

[6] E.M. Dannenberg, Rubber Chem. Technol., 48, 410 (1975)

[7] J.A.C. Harwood, A.R. Payne and J.F. Smith, Rubber Chem. Technol., 43, 687 (1970).

[8] A.I. Medalia, Rubber Chem. Technol., 45, 1171 (1972).

[9] C.J. Derham and A.G. Thomas, Rubber Chem. Technol., 50, 397 (1977).

[10] G.B. McKenna and R.W. Penn, J. Biomed Matls. Res., 14, 689 (1980).

[11] T.L. Smith, J. Polym. Sci., A, 1, 3597 (1963).

[12] T.L. Smith and R.A. Dickie, Rubber Chem. Technol. 43, 714 (1970) also J. Polym. Sci., A-2, 7, 635 (1969).

[13] T.L. Smith, J. Polym. Sci., 32, 99 (1958).

[14] T.L. Smith, as cited by R.F. Fedurs in "Uniaxial Rupture of Elastomers" in "The Stereo Rubbers", ed. by W.M. Saltman, John Wiley and Sons, New York (1977).

[15] T.L. Smith, "Strength and Extensibility of Elastomers", in "Rheology", Vol. 5, ed. by F.R. Eirich, Academic Press, New York (1969).

[16] D.R. Lesuer, A. Goldberg and J. Patt, in "Computer Modeling of Tank Track Elastomers", in "Elastomers and Rubber Technology", ed by R.E. Singler and C.A. Byrne, Sagamore Army Materials Research Conference Proceedings, 32, 211 (1987). (U.S. Gov't Printing Office, Washington, D.C., 1987).

[17] R.F. Fedors, "Uniaxial Rupture of Elastomers" in "The Stereo Rubbers", ed. by W.M. Saltman, John Wiley and Sons, New York (1977) p. 679.

Table 3-1. Compounding Formulations for Filled Rubber Compounds

Ingredients	Quantity, parts by mass	
	Butyl Rubber*	
NBS 388j, butyl rubber	100.00	
kNBS 370e, zinc oxide	3.00	
NBS 371g, sulfur	1.75	
NBS 372h, stearic acid	1.00	
NBS 378b, HAF black	50.00	
NBS 374c, tetramethylthiuram disulfide	1.00	
	15TP-14AX**	
SBR 1500	35.00	
Polybutadiene (98% Cis)		30.00
Natural Rubber (SMR20)	35.00	
N220 Carbon Black		65.00
Zinc Oxide	3.00	
Stearic Acid	1.50	
Waxy hydrocarbon blend (MP=65-70°C, SpGr=0.9-0.93)	1.50	
3-Dimethylbutyl-N'-phenyl-p-phenylene-diamine	3.00	
Polymerized 2,2,4-trimethyl-1, 2-dihydroquinoline	2.00	
High Aromatic Oil, ASTM D2226, type 102	4.00	
N-diisopropyl-2-benzothiazyl-sulfenamide	3.20	
Sulfur	1.30	
N-(cyclohexylthio)phthalimide		0.20
	NAT-25A**	
Natural Rubber, RSS-1	100.00	
Zinc Oxide	4.00	
Stearic Acid	2.00	
SAF Black N110	45.00	
Polytrimethyl dihydroquinoline	0.50	
di-β-naphthyl-p-phenylene diamine	0.50	
VANOX MTI	0.50	
N,N'-di-3(5-methyl heptyl)-p-phenylene diamine	5.00	
Sulfur, rubber makers	0.75	
Butyl Tuads		0.625
Octoate Z	1.5	
Amyl Ledate		1.0
AMAX	1.875	
	15TP-R	
Compound Formulation Unknown		

* Prepared according to ASTM D-3188-73, formula 1A.
** Prepared per ASTM D3182.

Table 3-2. Parameters from Least Squares Analysis of Equation 2* from Fatigue Failure Data for 15TP-14AX and 15NAT-25A Rubber Compounds

	Parameter	Value**
15TP-14AX	Log A	6.873 ± (0.146)
	γ	-0.688 ± (0.016)
	β	-3.532 ± (0.138)
15NAT-25A	Log A	4.591 ± (0.324)
	γ	-0.784 ± (0.037)
	β	-2.501 ± (0.341)

* $t_f = A\omega^{\gamma}\sigma^{\beta}$

** Numbers in parentheses represent approximate standard deviation on the parameter value.

Table 3-3. Formulation for Proposed Nitrile Rubber Compound

Ingredient	pph
Chemigum N-615*	100.00
Zinc Oxide	5.00
Stearic Acid	1.00
HAF Black	50.00
Altax	2.00
Methyl Tuads	1.00
Spider Brand Sulfur	0.30

*Butadiene-acrylonitrile copolymer having 31-34% bound acrylonitrile

Table 3-4. Formulations for Proposed Sulfur Cured and Proposed Peroxide Cured EPDM Rubber Compounds

	Ingredient	pph
Surfur Cured:	Epsyn 70A	50.0
	Epsyn 5508	50.0
	HAF Black	50.0
	Circosal 4240	30.0
	Stearic Acid	0.5
	Mercaptobenzothiazole	0.5
	Unads	1.0
	Sulfur	1.0
	Zinc Oxide	5.0
Peroxide Cured:	Epsyn 40A	100.0
	Vulcan 3	60.0
	Circosal 4240	10.0
	Zinc Oxide	5.0
	Agerite Resin D	1.0
	Di Cup 40C	8.5

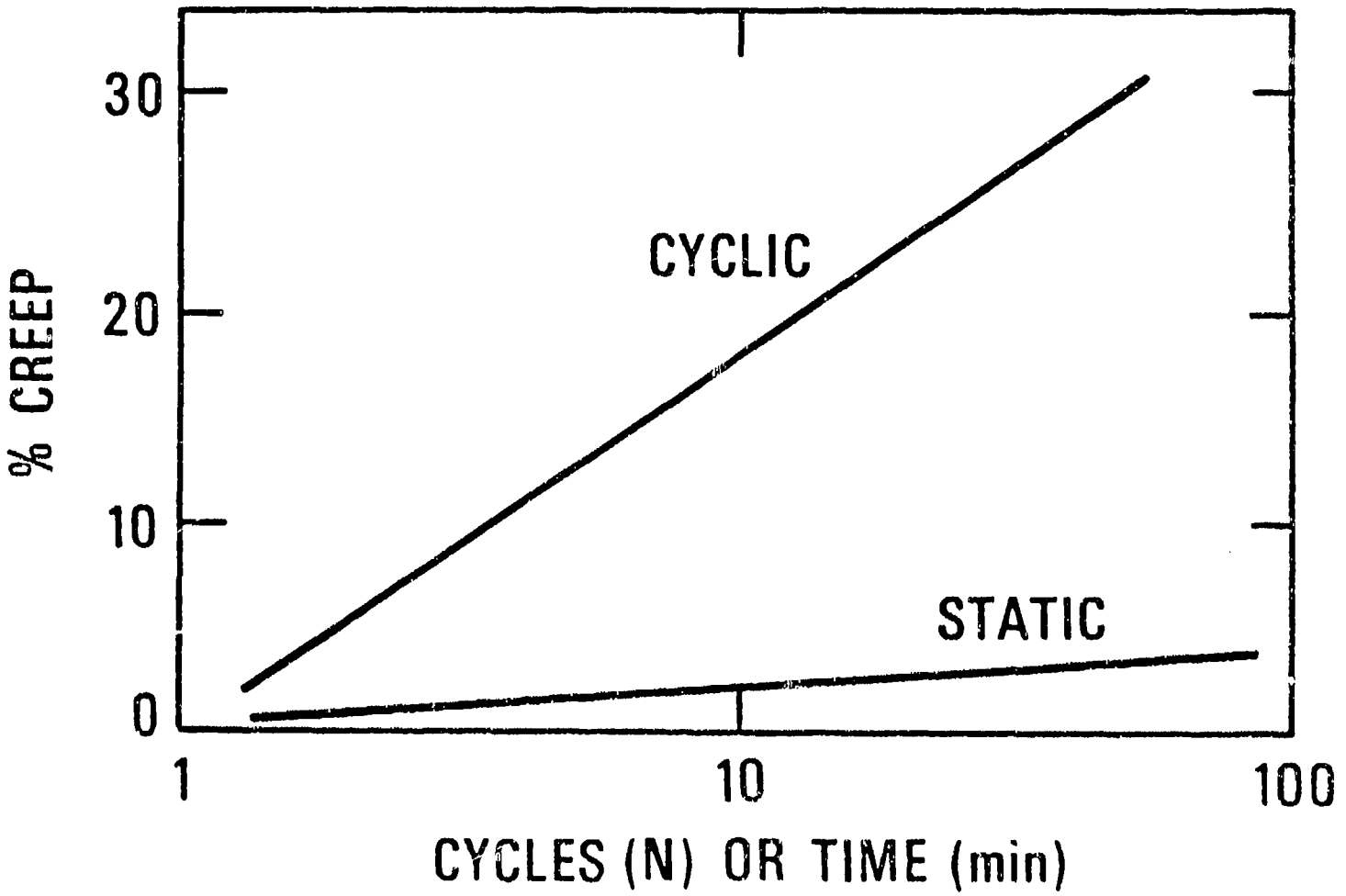

C.J. Derham and A.G. Thomas, 1976

Figure 3-1 Schematic of the differences in creep behavior of a filled natural rubber in creep and static loading [after Derham and Thomas (9)].

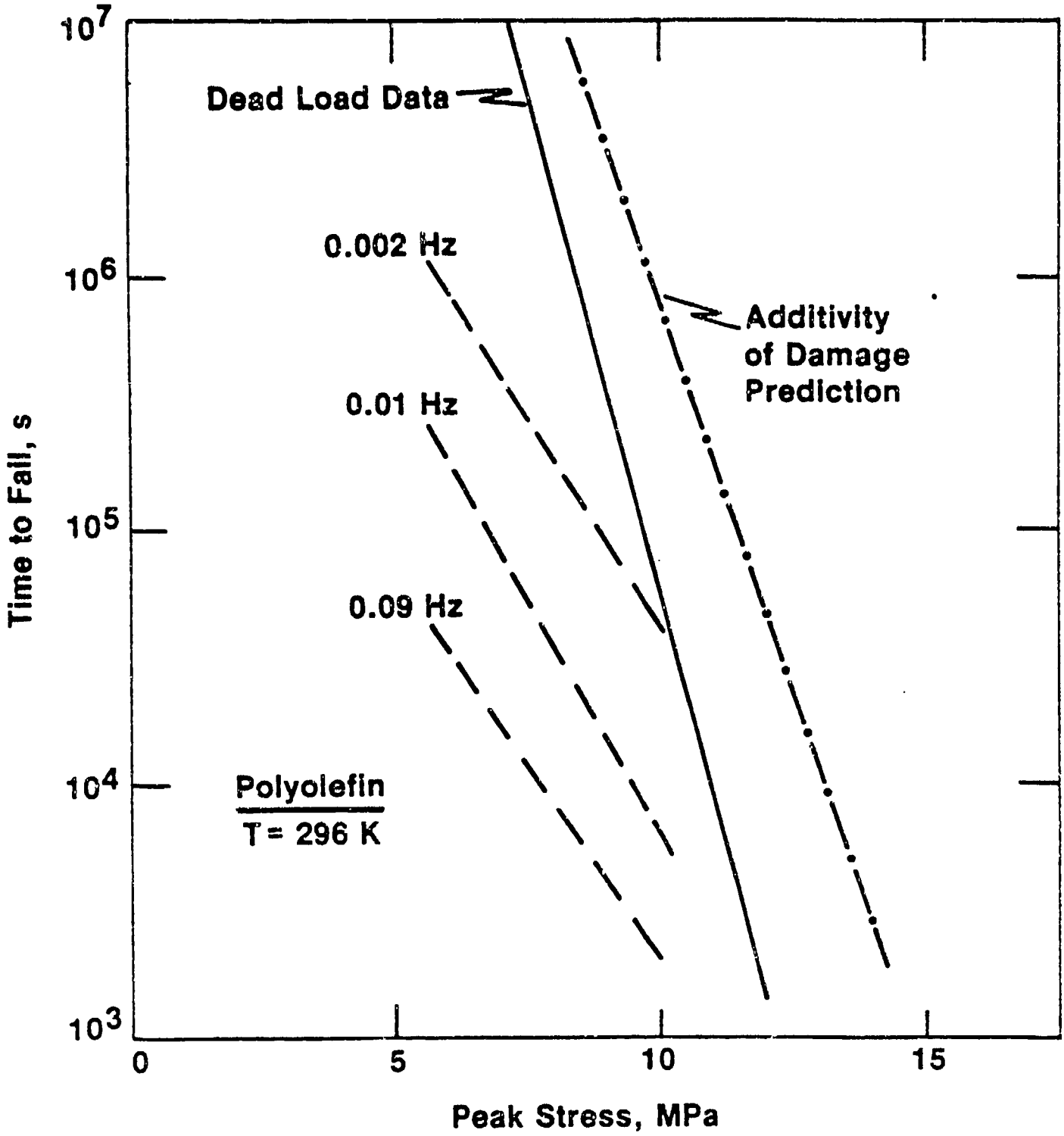

Figure 3-2 Lifetime vs (peak)stress for a filled polyolefin rubber comparing fatigue behavior with static behavior and prediction of fatigue lifetime from a cumulative damage law [after McKenna and Penn(10)].

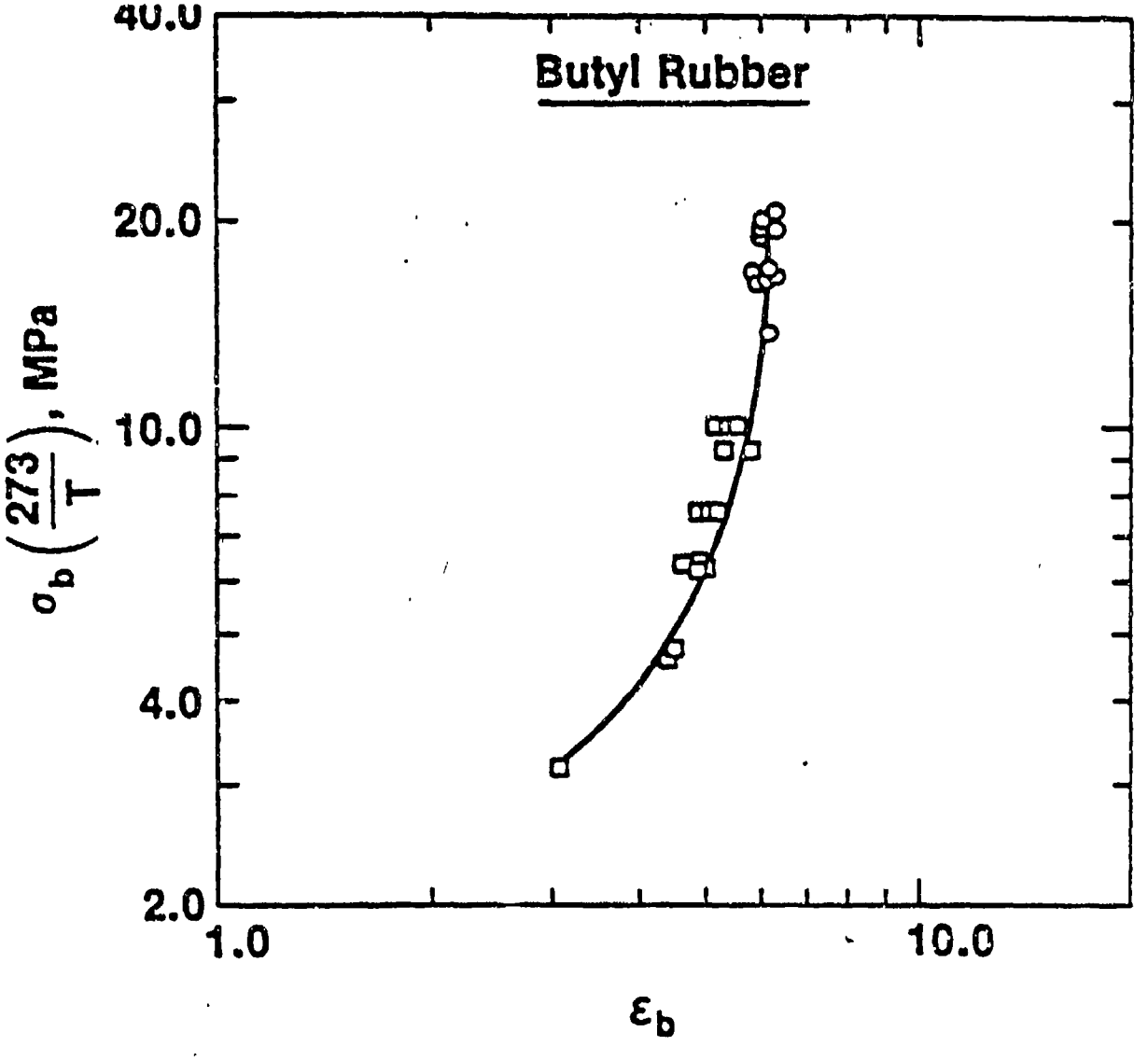

Figure 3.3 Typical failure envelope for a carbon black filled butyl rubber. (o) From constant rate of deformation measurements. (□) From creep to failure measurements. [After McKenna and Zapas(2).]

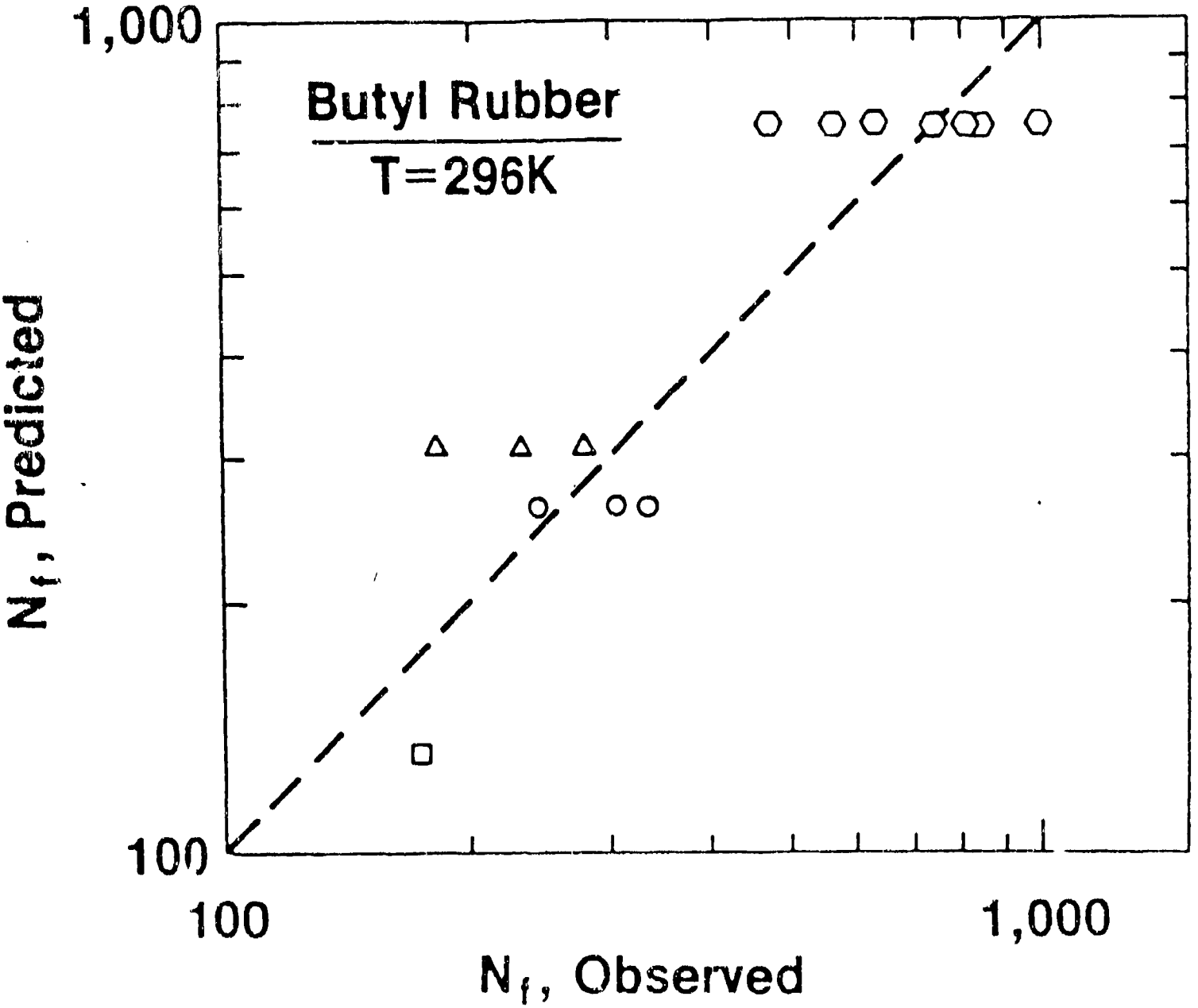

Figure 3-4 Comparison of number of cycles to failure predicted from cycle shifted failure envelope (CSFE) model with observed number of cycles to failure for a filled butyl rubber at a peak stress of 5.5 MPa(800 psi). Zero-tension loading. Sinusoidal: (□) 0.0002 Hz; (○) 0.01 Hz; ( ) 0.09 Hz. Squarewave: (Δ) Symmetric with 52.4s period. [After McKenna and Zapas (2).]

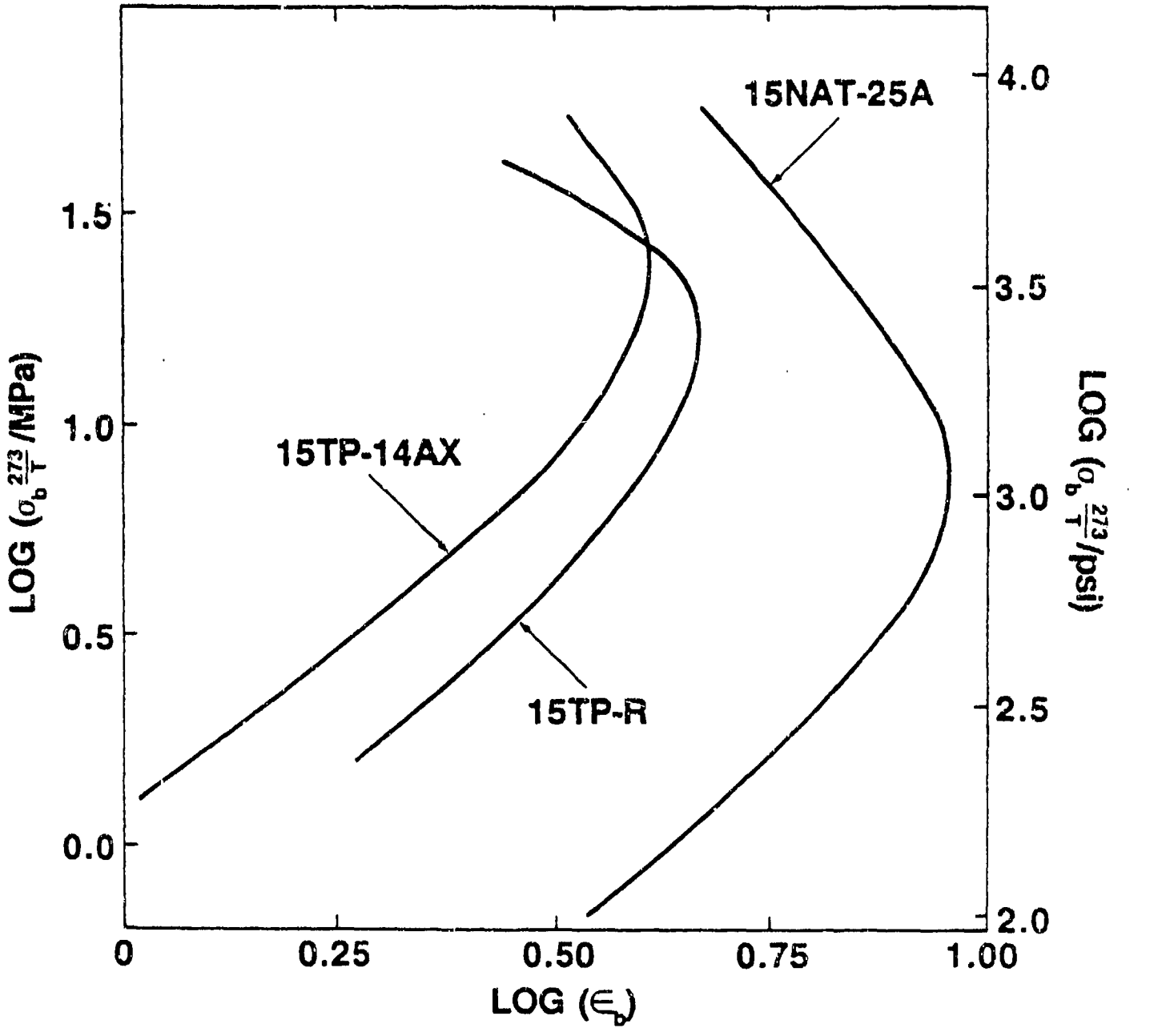

Figure 3-5 Comparison of failure envelopes obtained from constant rate of deformation experiments for three tank track rubber compound as indicated. [After McKenna (1).]

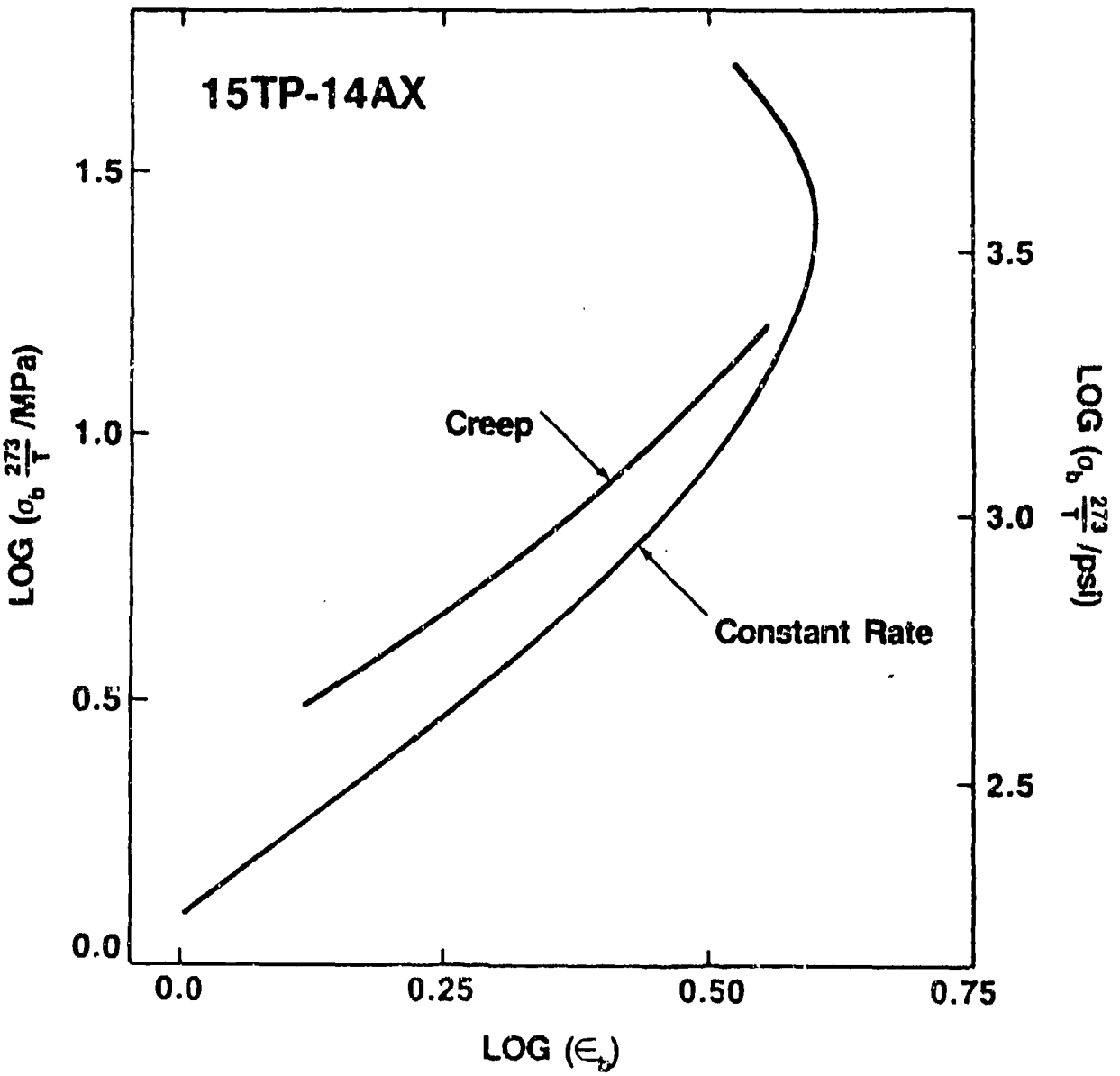

Figure 3-6 Comparison of failure envelopes for 15TP-14AX rubber compound obtained from constant rate of deformation and creep experiments, as indicated. [After McKenna (1).]

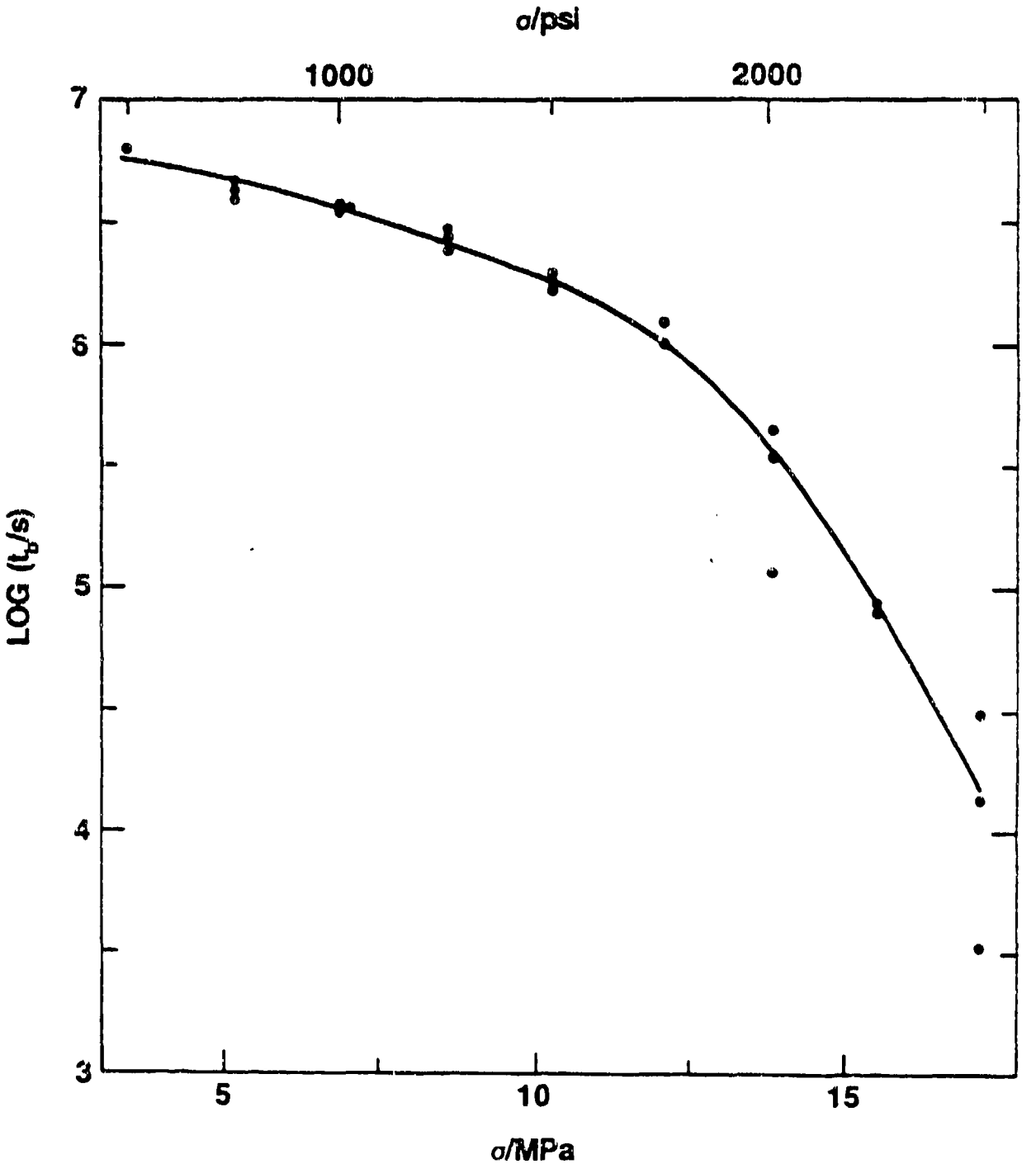

Figure 3-7 Semilogarithmic depiction of time-to-failure vs applied (engineering) stress for 15TP-14AX rubber compounds in creep experiments at 23°C. [After McKenna (1).]

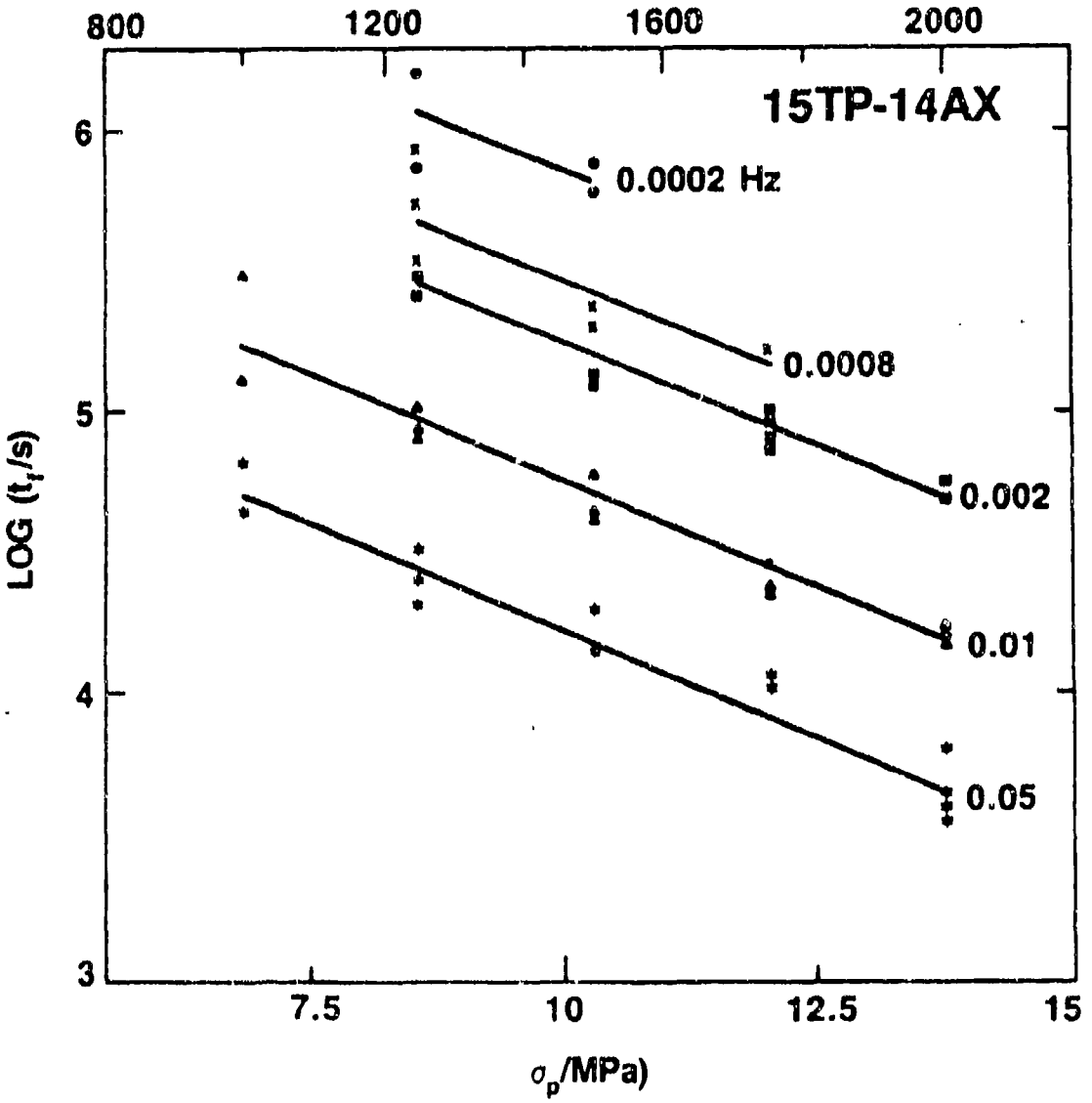

Figure 3-8 Semilogarithmic depiction of time-to-failure vs peak (engineering) stress in zero tension sinusoidal loading for 15TP-14AX rubber compound at different test frequencies, as indicated. [After McKenna (1).]

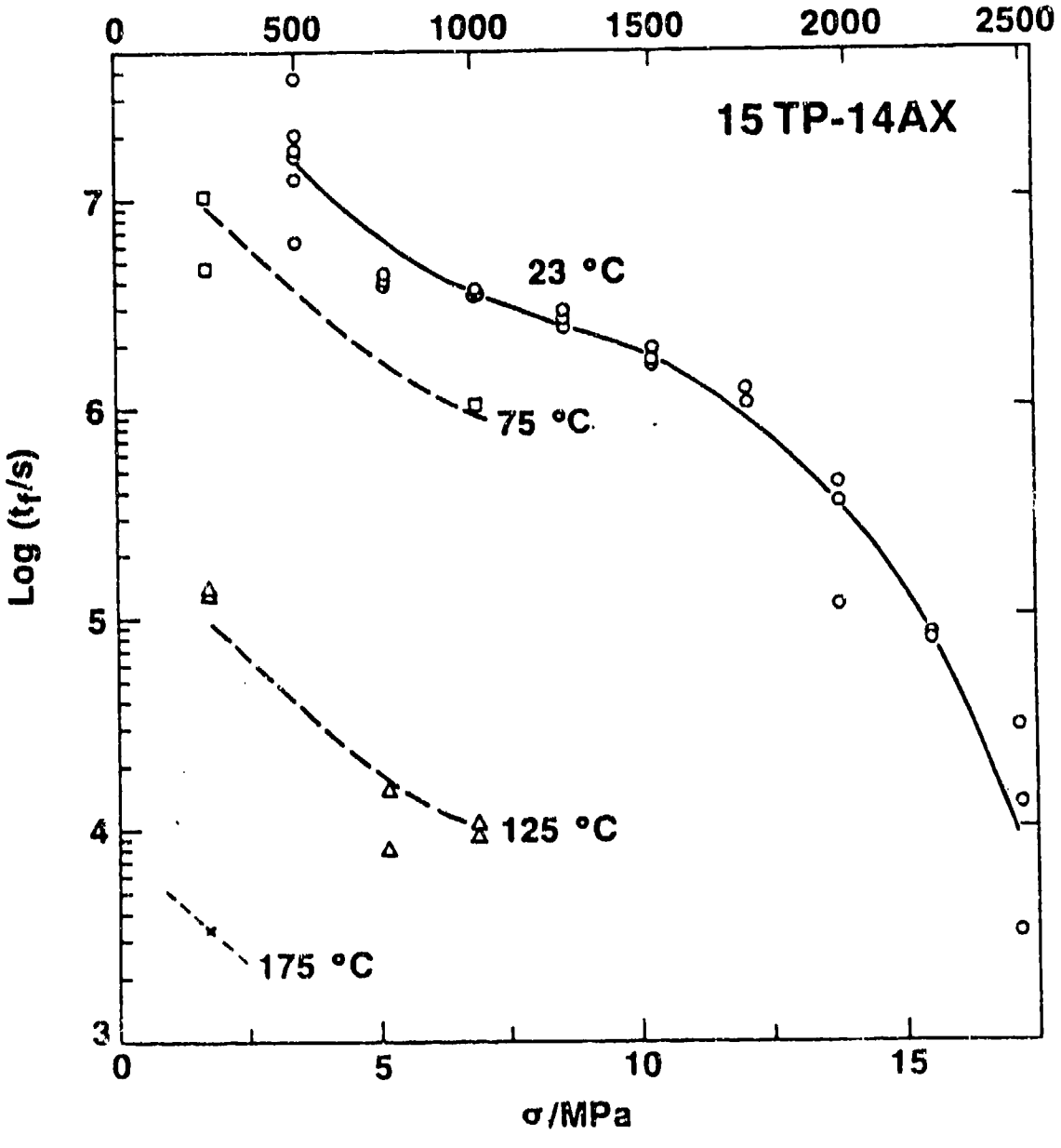

Figure 3-9 Semilogarithmic depiction ofthe time-to-failure vs applied (engineering) stress for 15TP-14AX rubber compound under constant loading conditions at 23°, 75°, 125° and 175°C as indicated. Dashed lines drawn assuming stress dependence of lifetime is independent of temperature.

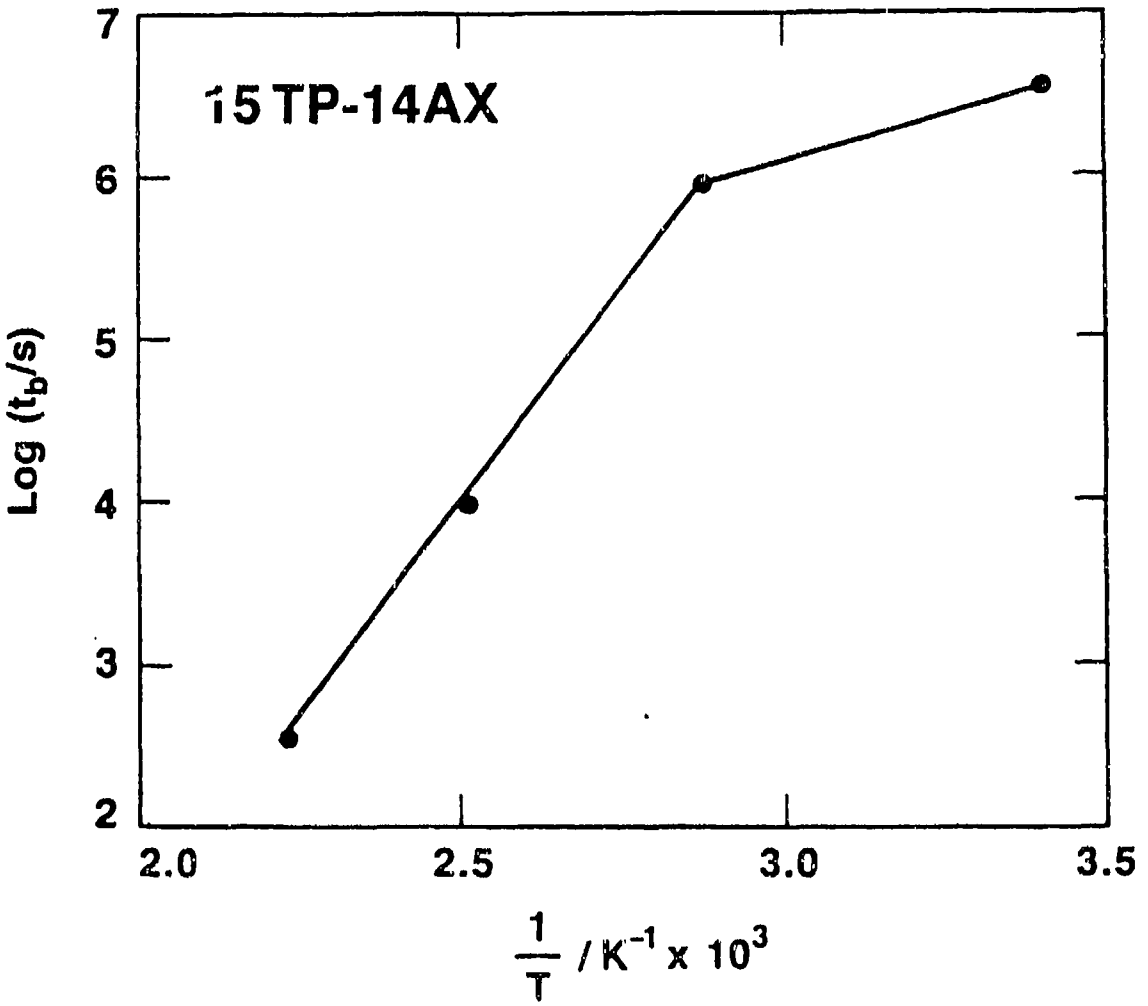

Figure 3-10 Logarithm of failure time vs 1/T for 15TP-14AX rubber in constant loading conditions.

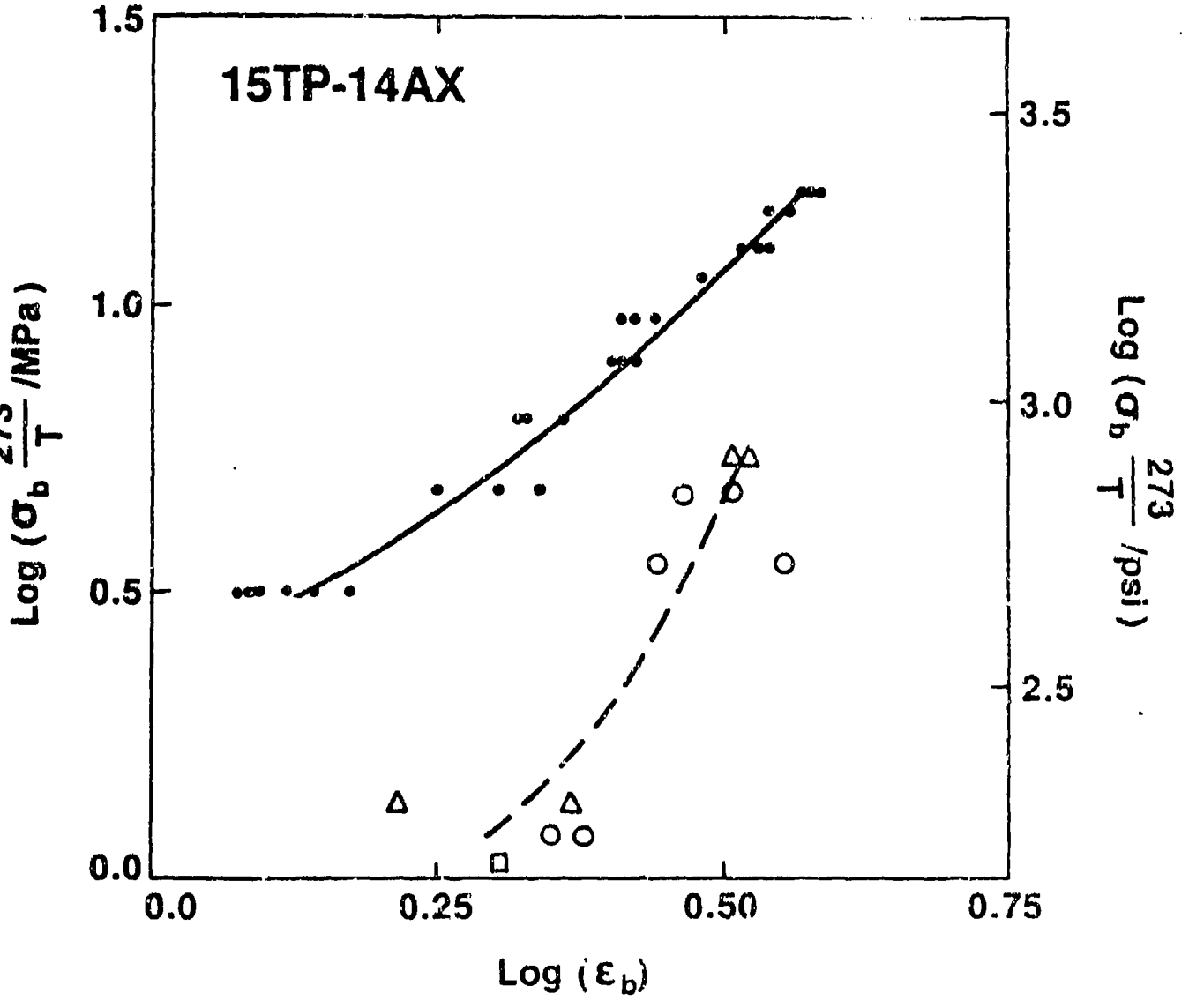

Figure 3-11 Failure envelopes for 15TP-14AX obtained in creep experiments. Solid line: "low temperature" envelope; dashed line: "high temperature" envelope. Points for data taken at different temperatures: (•) 23°C; (Δ)75°C; (o) 125°C; (□) 175°C.

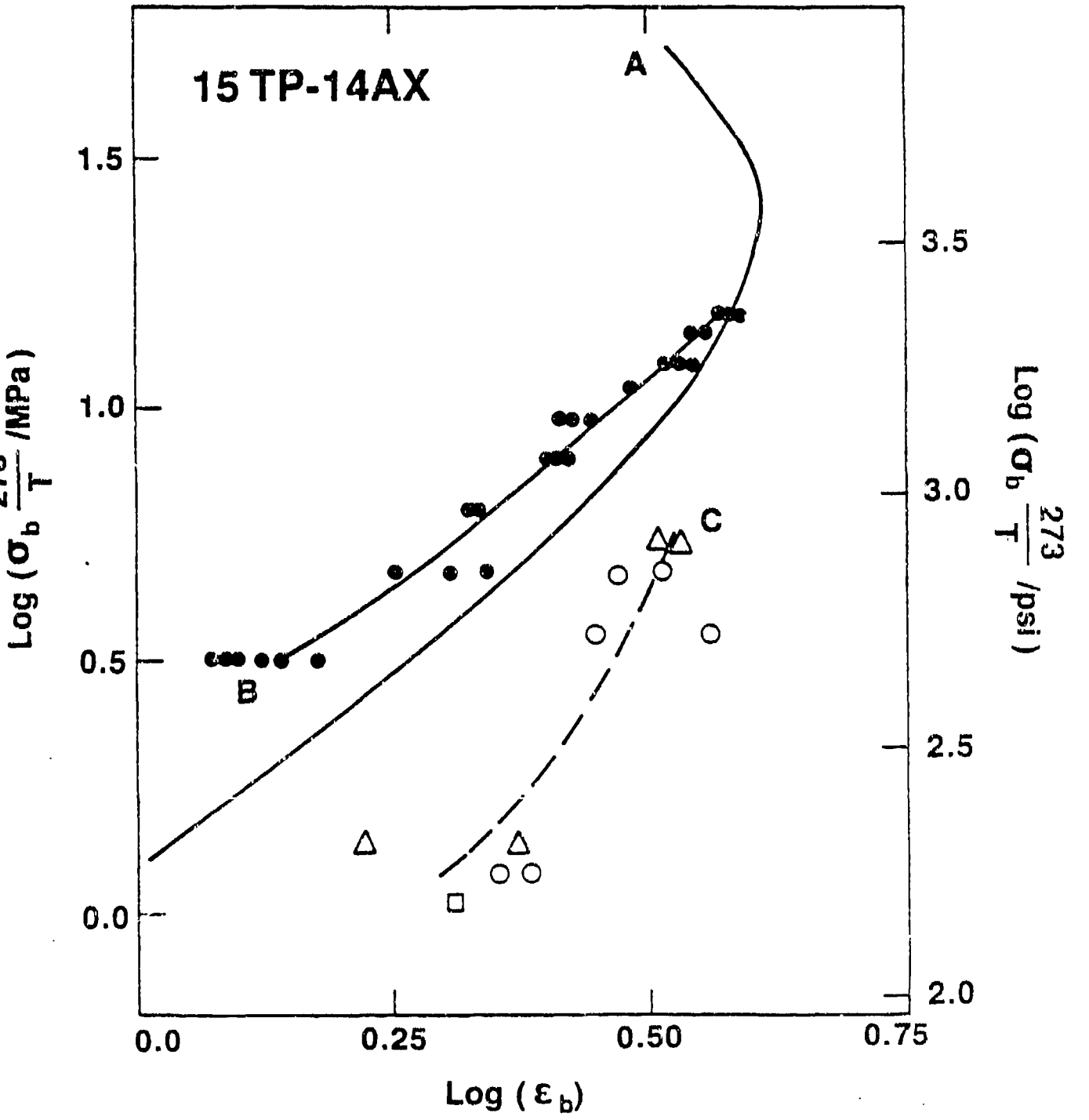

Figure 3-12 Comparison of Failure envelopes for 15TP-14AX rubber compound. (A) From constant rate of deformation experiments; (B) "low temperature" creep envelope; (C) "High temperature" creep envelope. Points as in Figure 3-11.

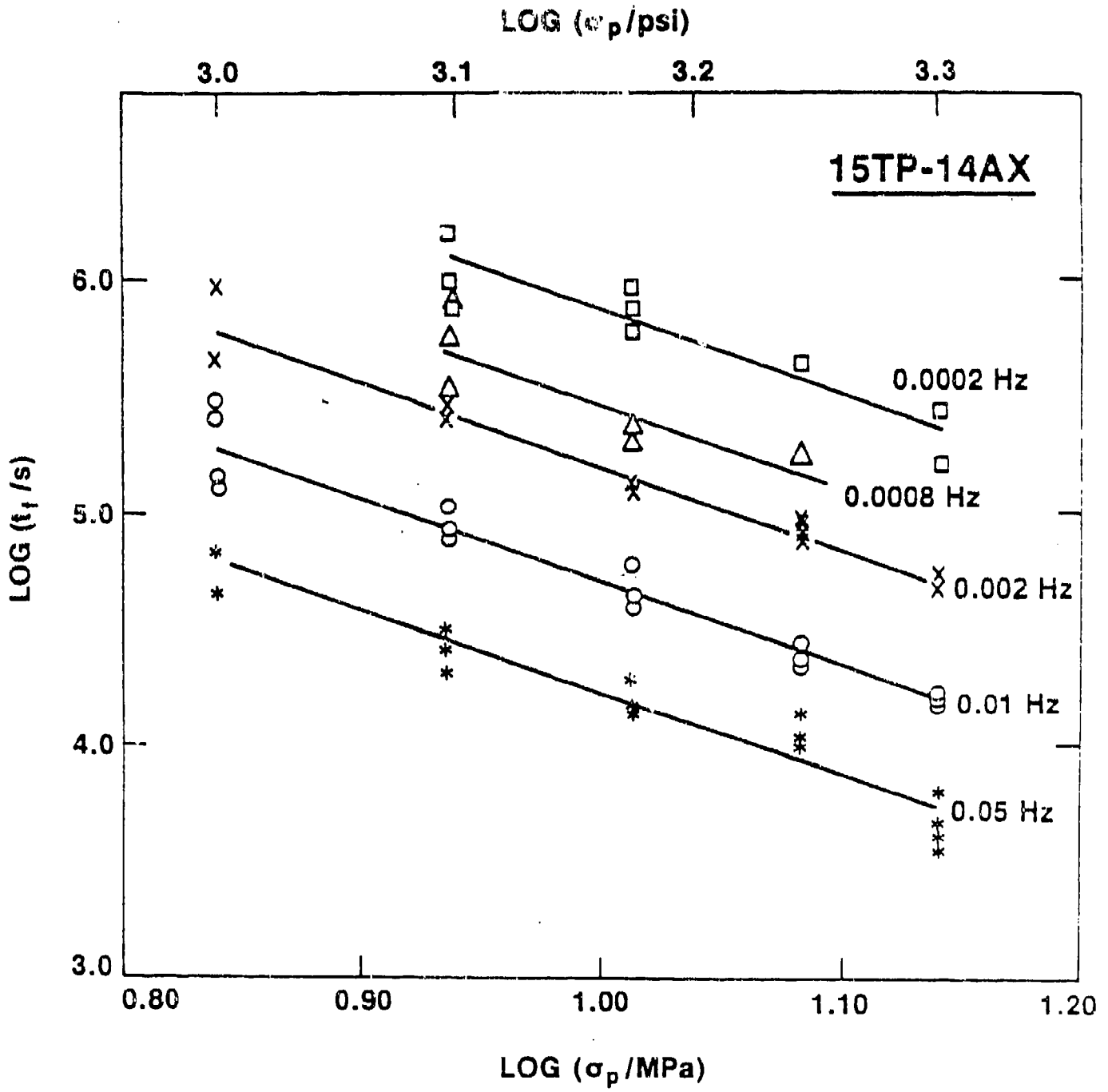

Figure 3-13 Double logarithmic representation of failure time vs peak (engineering) stress for 15TP-14AX rubber compound in zero-tension sinusoidal loading at different test frequencies, as indicated. Lines from equation 2.

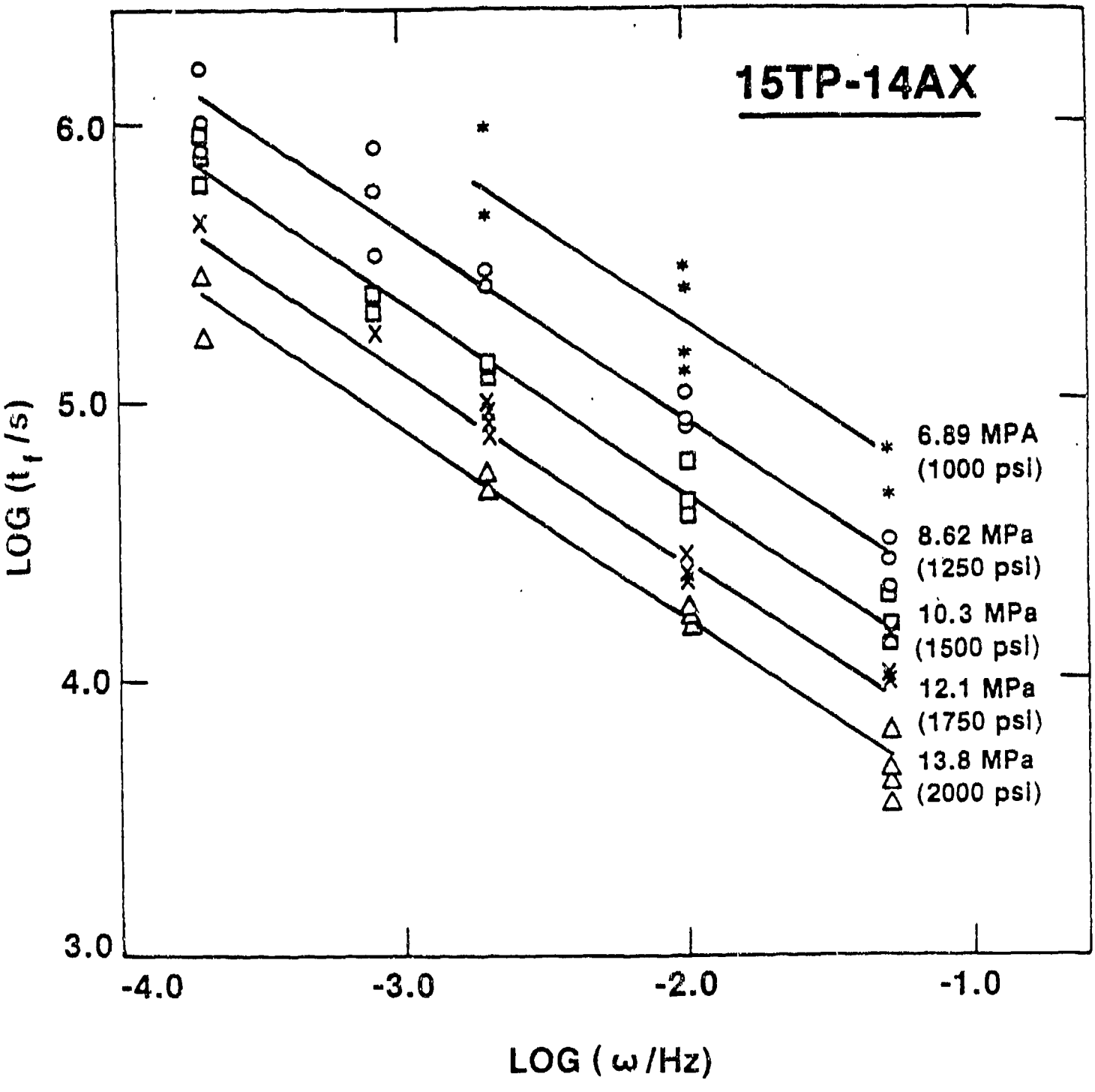

Figure 3-14 Double logarithmic representation of failure time vs test frequency for 15TP-14AX rubber compound in zero-tension sinusoidal loading at different stresses, as indicated. Lines from equation 2.

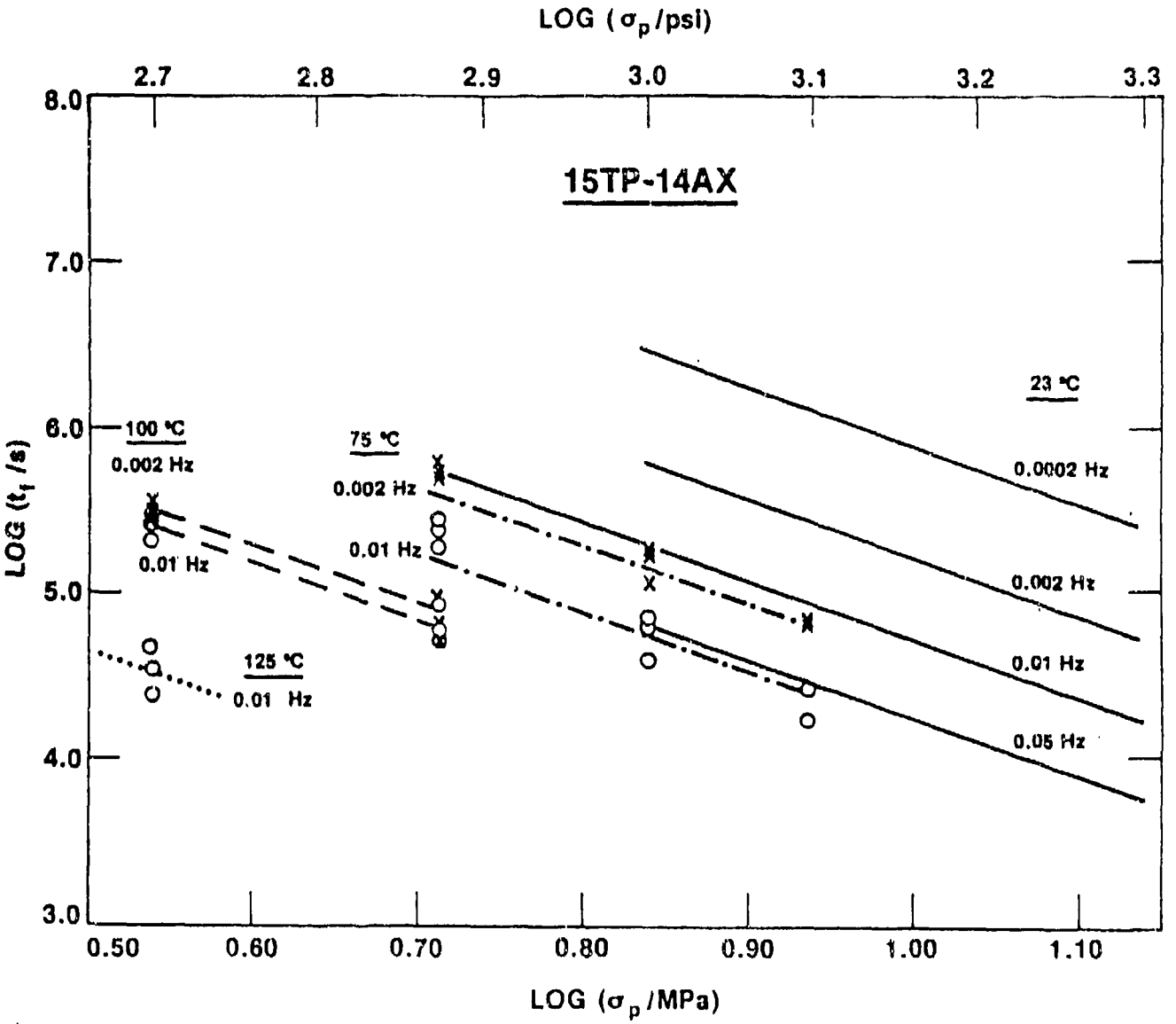

Figure 3-15 Double logarithmic representation of failure time vs peak stress for 15TP-14AX rubber compound in zero-tension sinusoidal loading at different test temperatures and frequencies, as indicated. Solid lines are for 23°C data from equation 2. Other lines drawn parallel to those at 23°C.

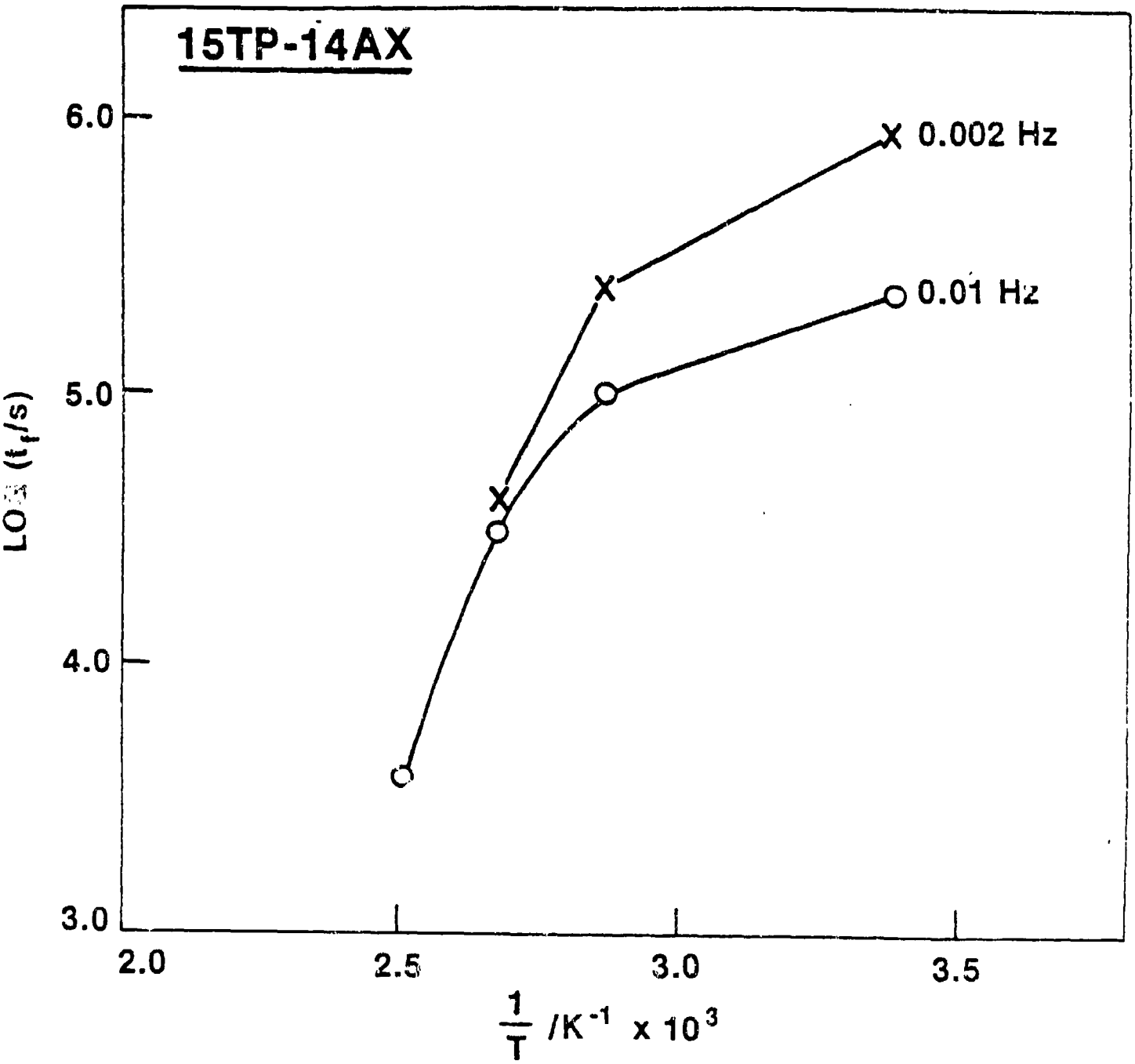

Figure 3-16 Logarithm of the time-to-failure vs 1/T for 15TP-14AX rubber compound in zero-tension sinusoidal loading at 0.002 and 0.01 Hz as indicated. σ_p = 6.2 MPa (900 psi).

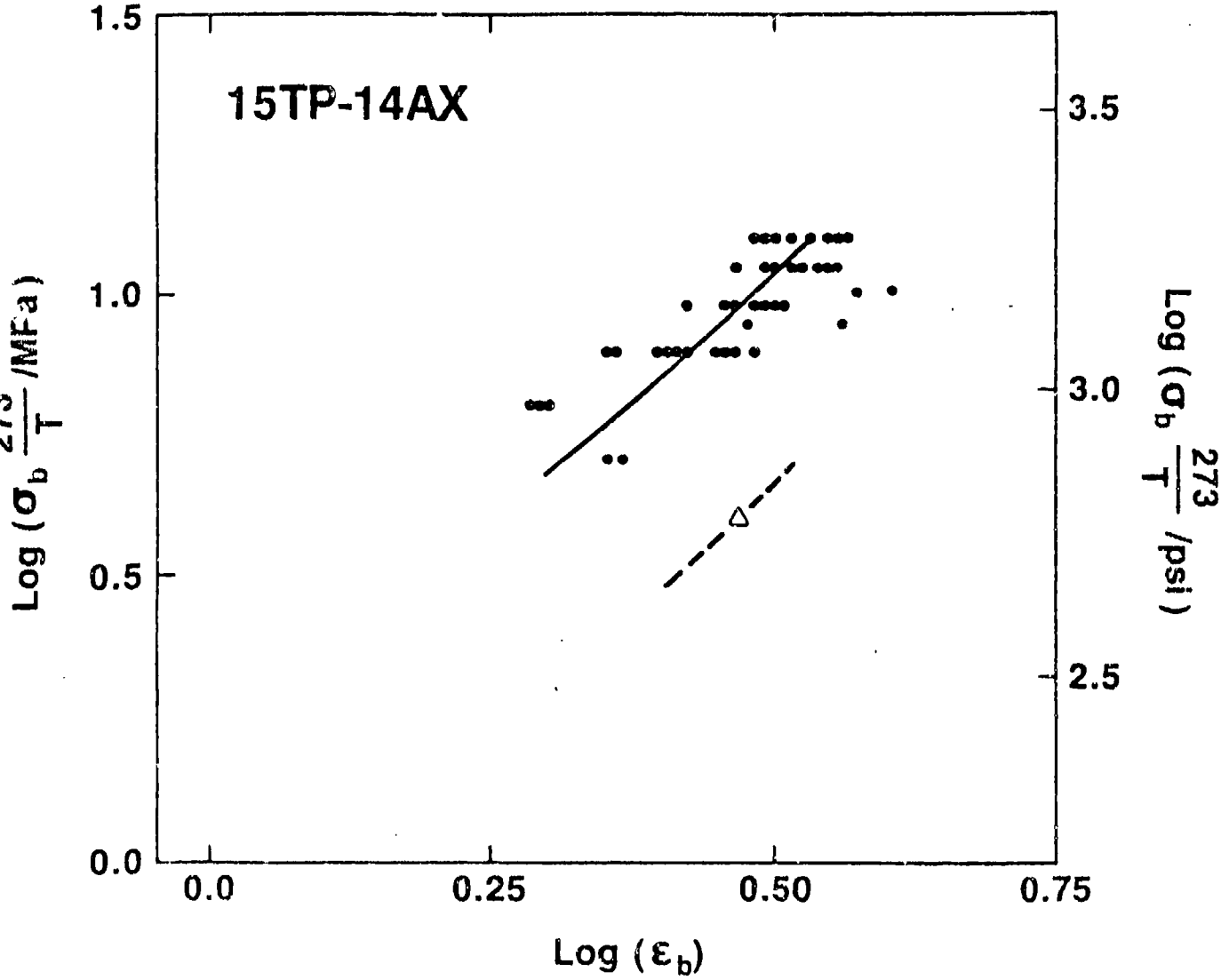

Figure 3-17 Fatigue failure envelopes for 15TP-14AX rubber compound. Solid line represents "low temperature" envelope, dashed line the "high temperature" envelope. (•) 23°C; (Δ) 75°C.

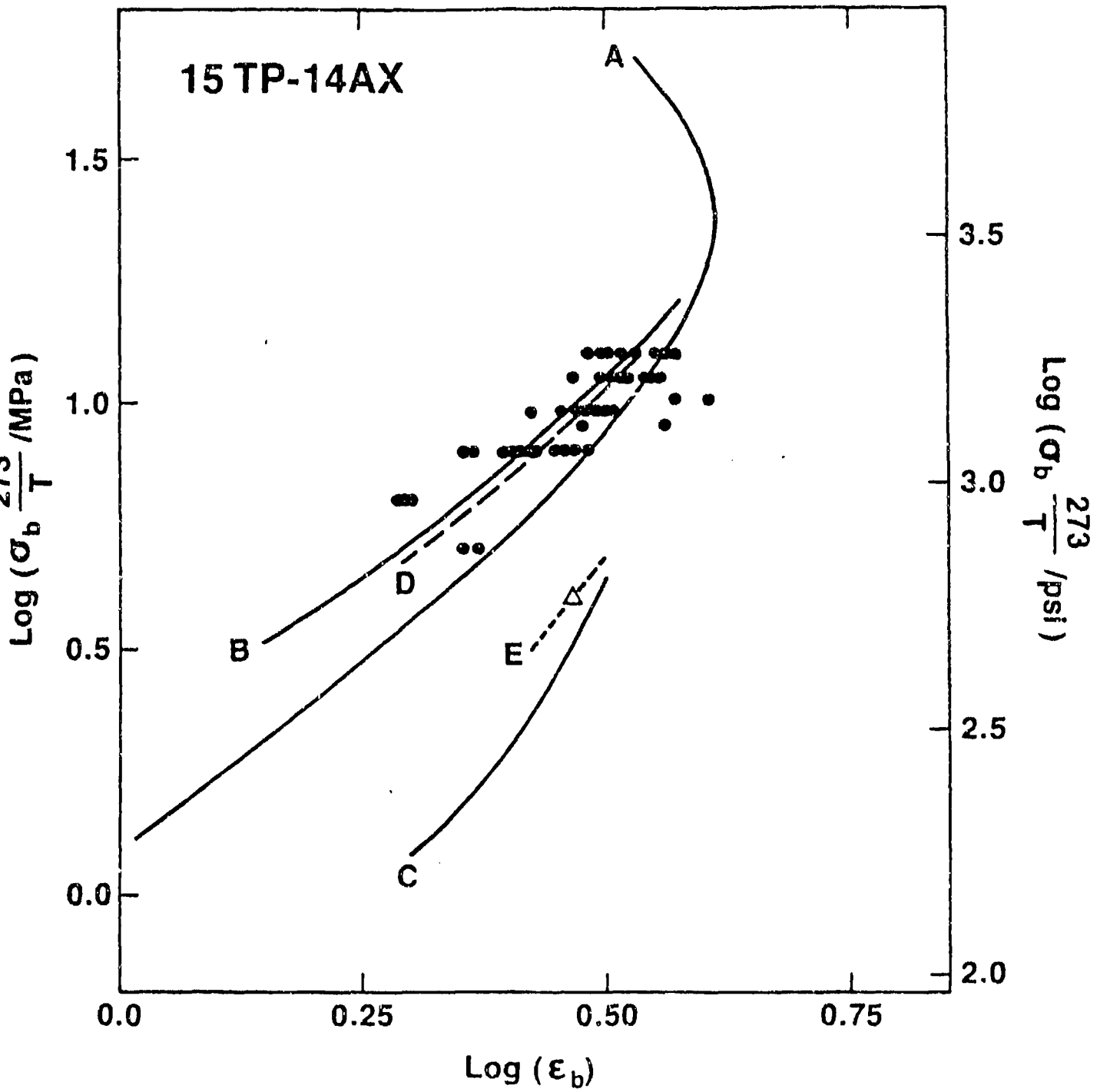

Figure 3-18 Comparison of failure envelopes obtained from different types of measurement for 15TP-14AX rubber compound. (A) constant rate of deformation; (B) "low temperature" creep; (C) "high temperature" creep; (D) "Low temperature" fatigure and (E) "high temperature" fatigue. Points are as in Figure 3-17.

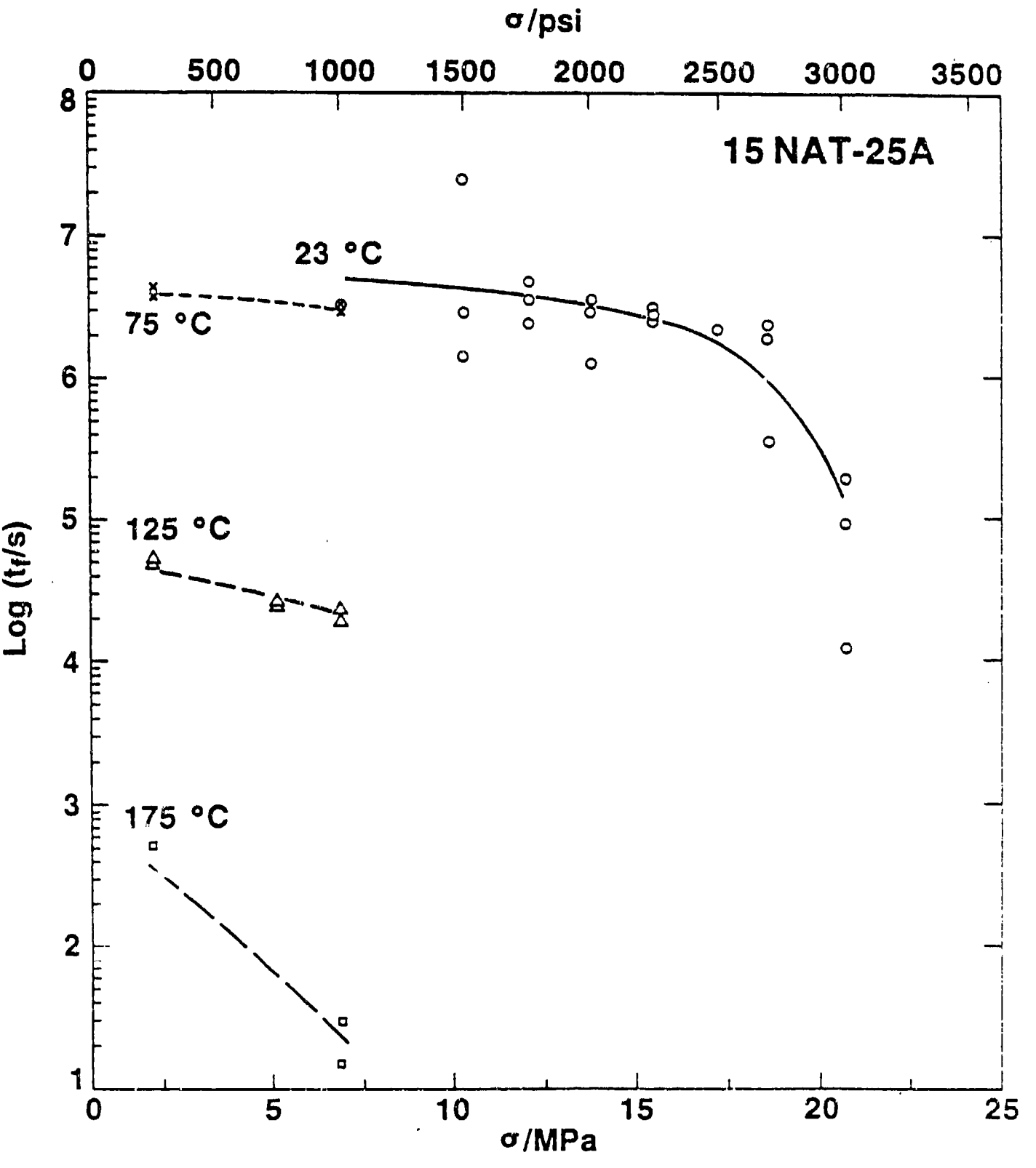

3-19 Semilogarithmic depiction of time-to-failure vs (engineering) stress for 15NAT-25A rubber compound under constant loading conditions at different temperatures, as indicated.

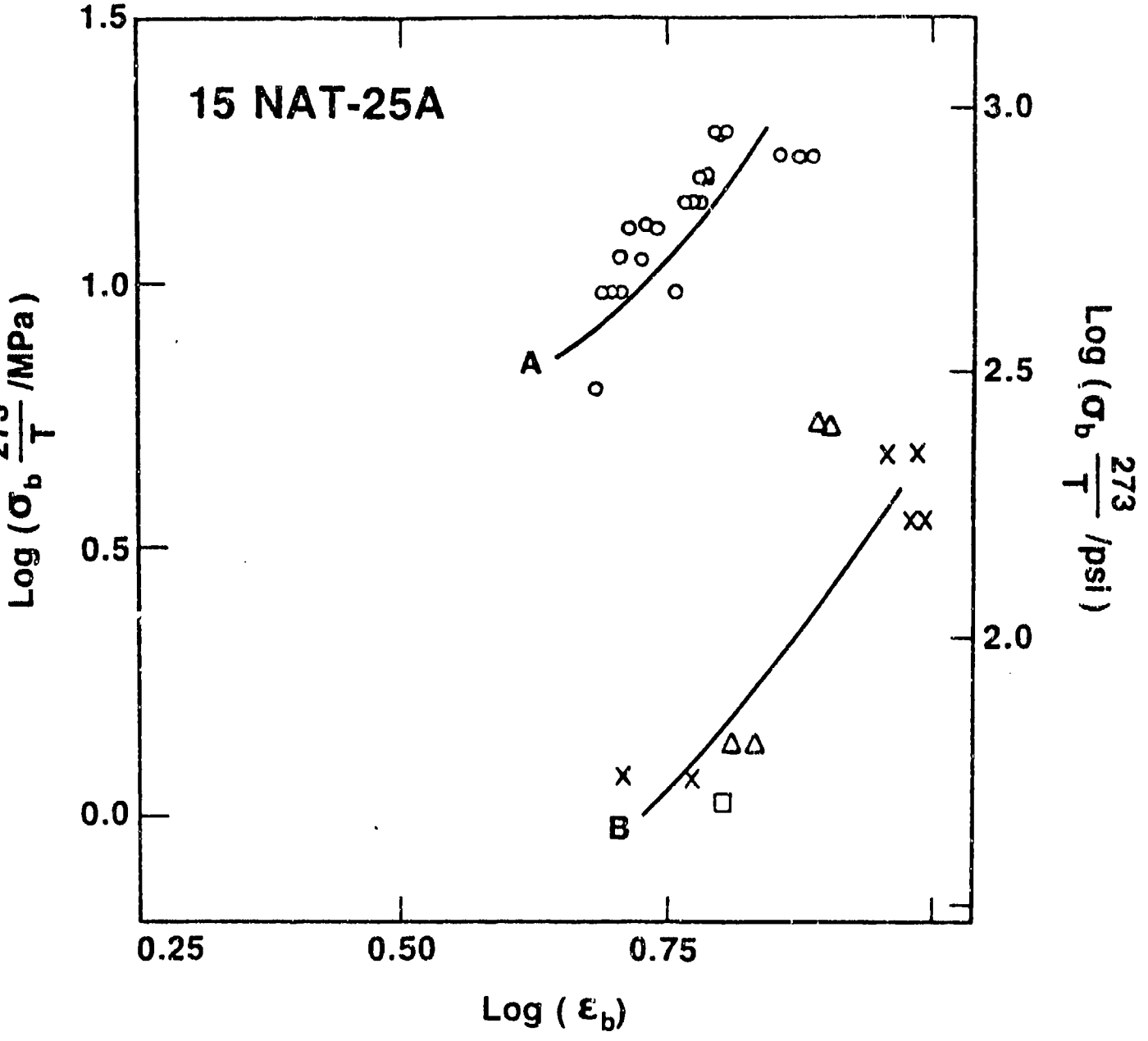

Figure 3-20 Creep failure envelopes for 15NAT-25A rubber compound. (A) "low temperature" envelope and (B) "high temperature" envelope (o) 23°C; (Δ) 75°C; (X) 125°C; (□) 175°C.

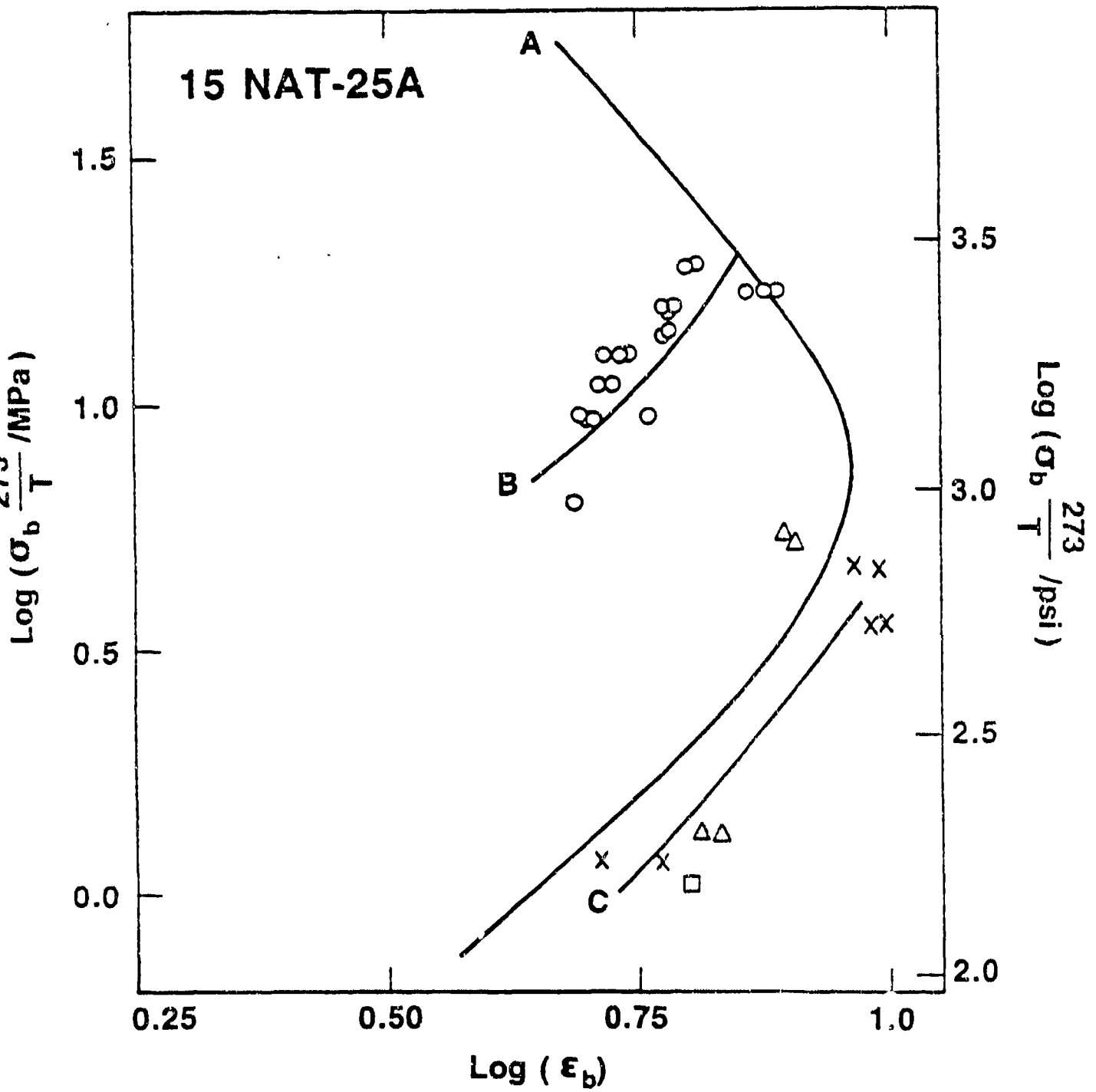

Figure 3-21 Comparison of constant rate and creep failure envelopes for 15NAT-25A rubber compound. (A) constant rate failure envelope; (B) "low temperature" creep envelope; (C) "high temperature" creep envelope. Points are as in Figure 3-20.

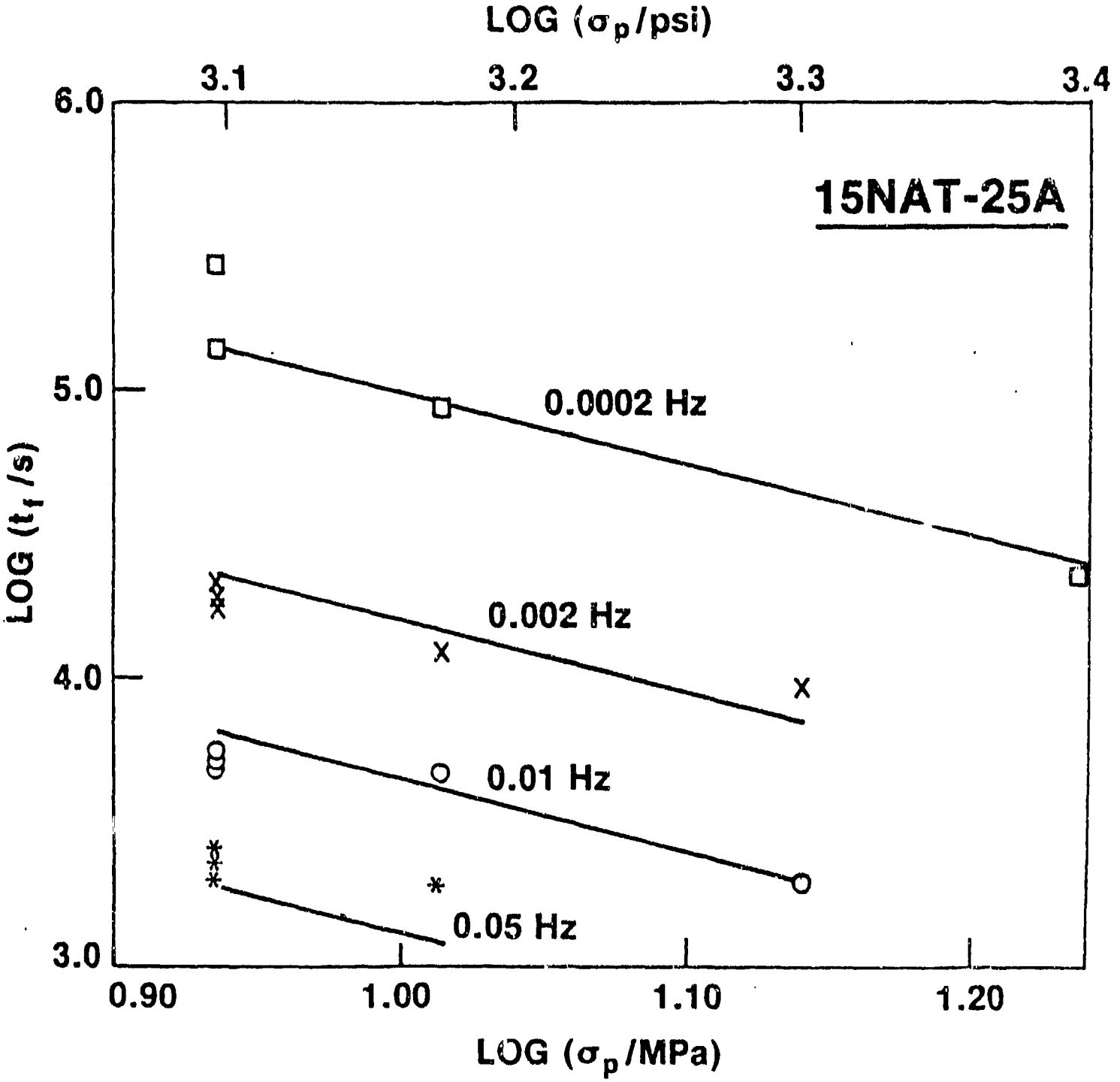

Figure 3-22 Double logarithmic representation of failure time vs peak stress for 15NAT-25A subjected to zero-tension sinusoidal loading at different test frequencies, as indicated. Points are data, lines represent least squares fit to equation 2.

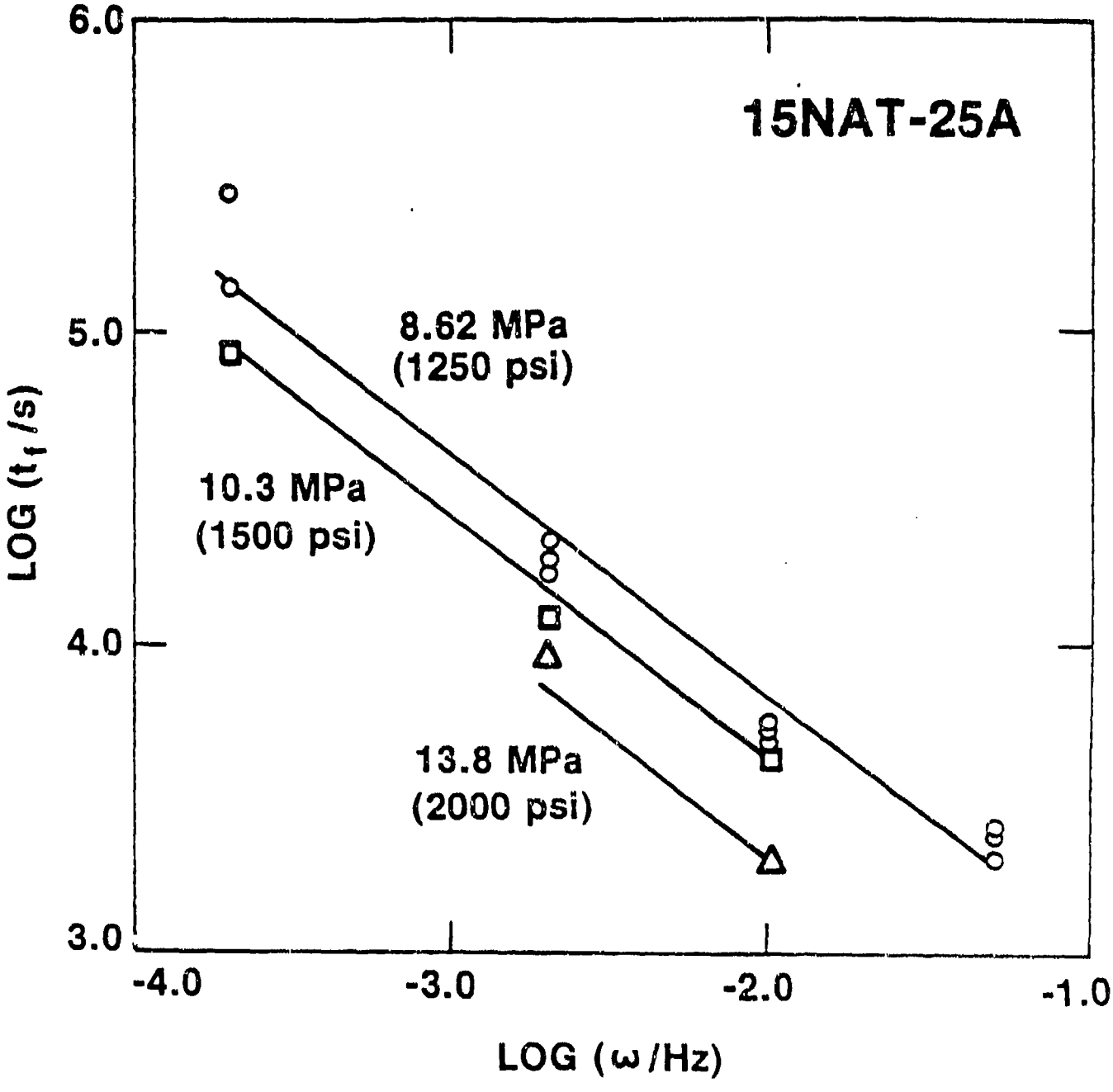

Figure 3-23 Double logarithmic representation of time-to-failure vs test frequency for 15NAT-25A rubber compound subjected to zero-tension sinusoidal loading at different peak stresses, as indicated. Points are data, lines represent least squares fit to equation 2.

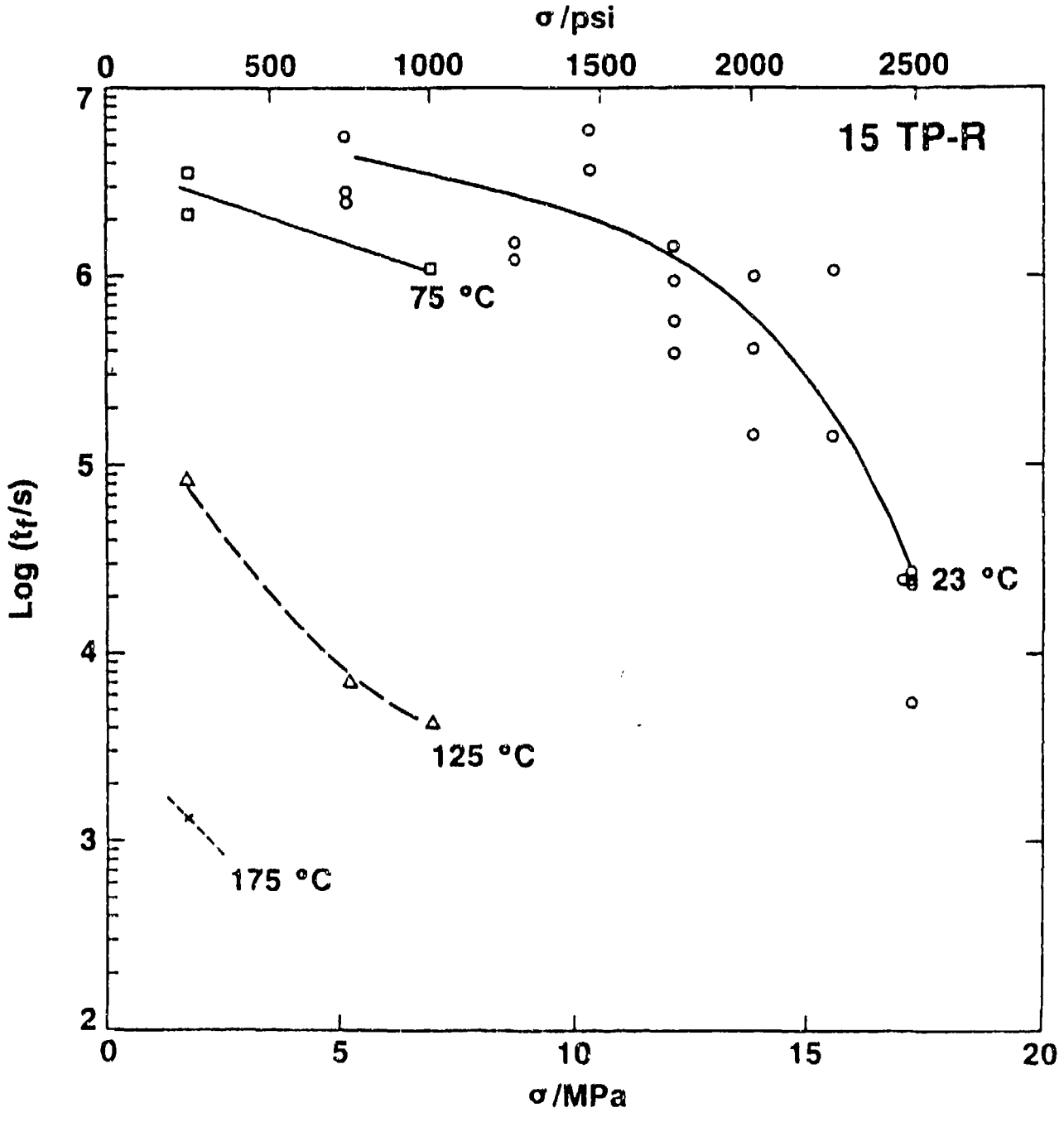

Figure 3-24 Semi-logarithmic representation of time-to-failure vs (engineering) stress for 15TP-R rubber compound at different temperatures, as indicated.

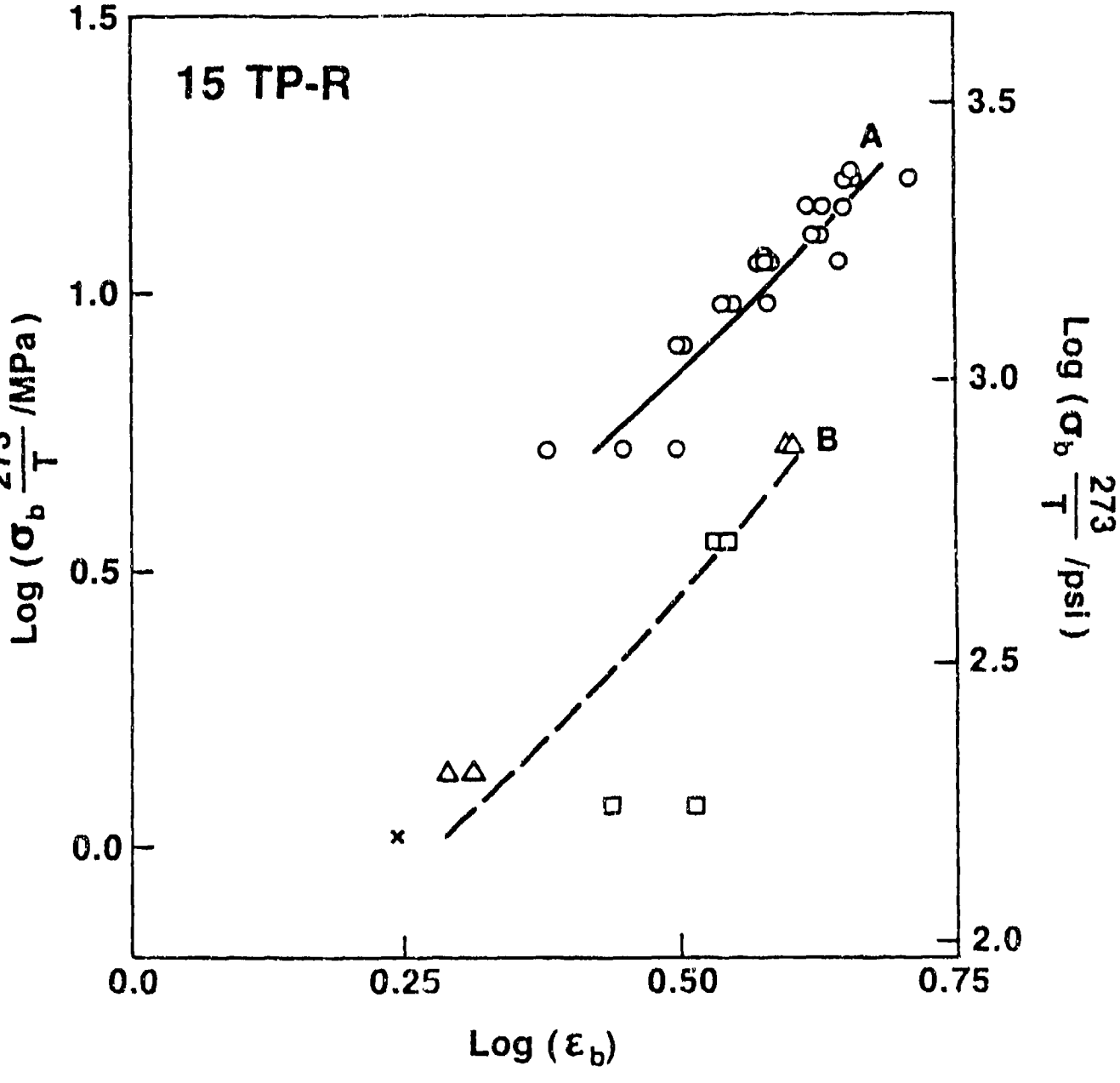

Figure 3-25 Failure envelopes obtained in creep loading conditions for 15TP-R rubber compound at (Δ) "low" and (B) "high" temperatures. (o) 23°C; (Δ) 75°C; (□) 125°C; (X) 175°C.

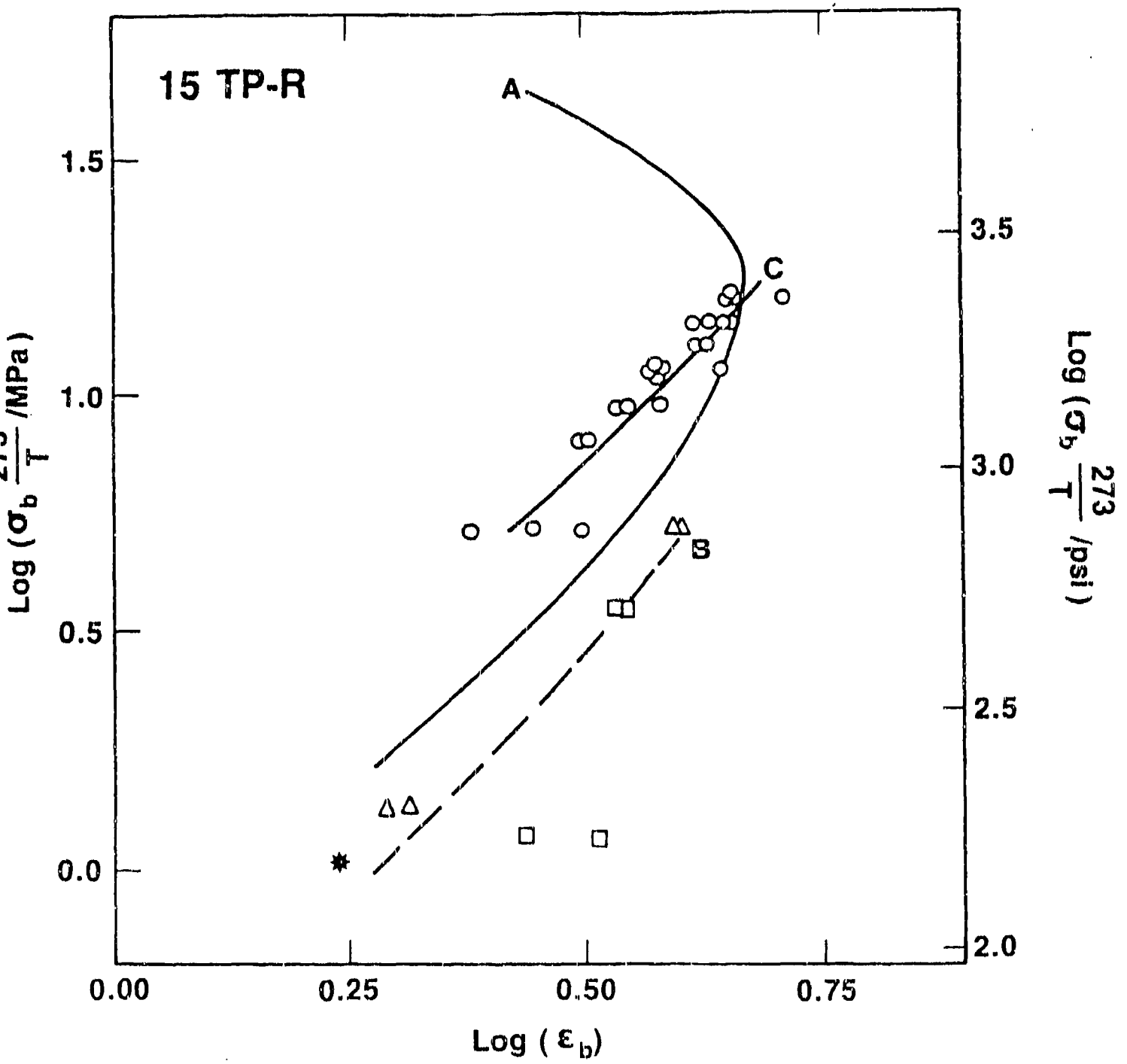

Figure 3-26 Comparison of creep and constant rate failure envelopes for 15TP-R rubber compound. (A) Constant rate of deformation envelope; (B) "high temperature" creep envelope; (C) "low temperature" creep envelope. Points as in Figure 3-25.

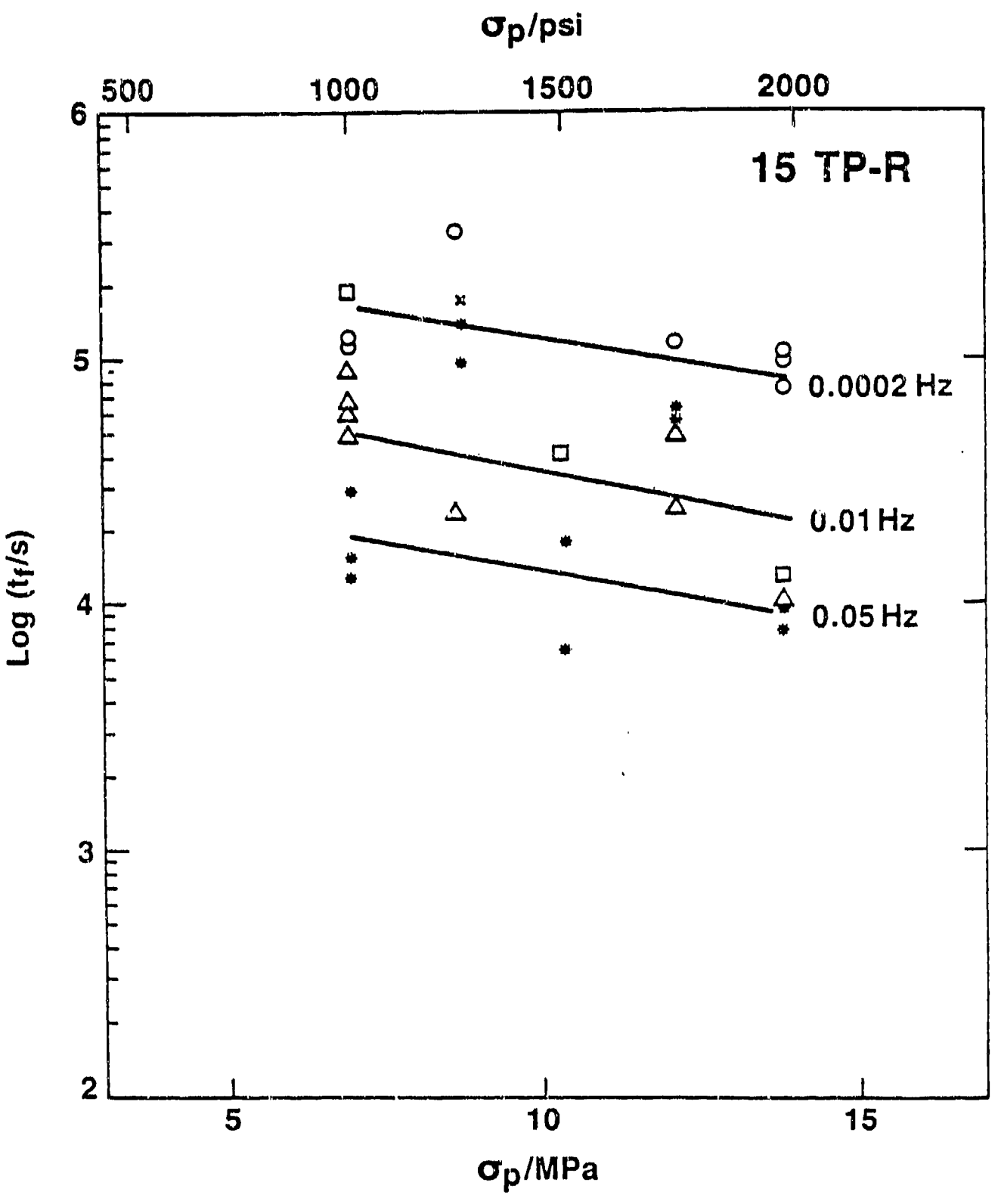

Figure 3-27 Semi-logarithmic depiction of time-to-failure vs peak stress for 15TP-R rubber compound subjected to different test frequencies at T = 23°C. Lines represent estimated behavior, large scatter in data must be emphasized here. Points represent actual data at different test frequencies: (o) 0.0002 Hz; (x) 0.0008 Hz; (□) 0.002 Hz; (Δ) 0.01 Hz; (*) 0.05 Hz.

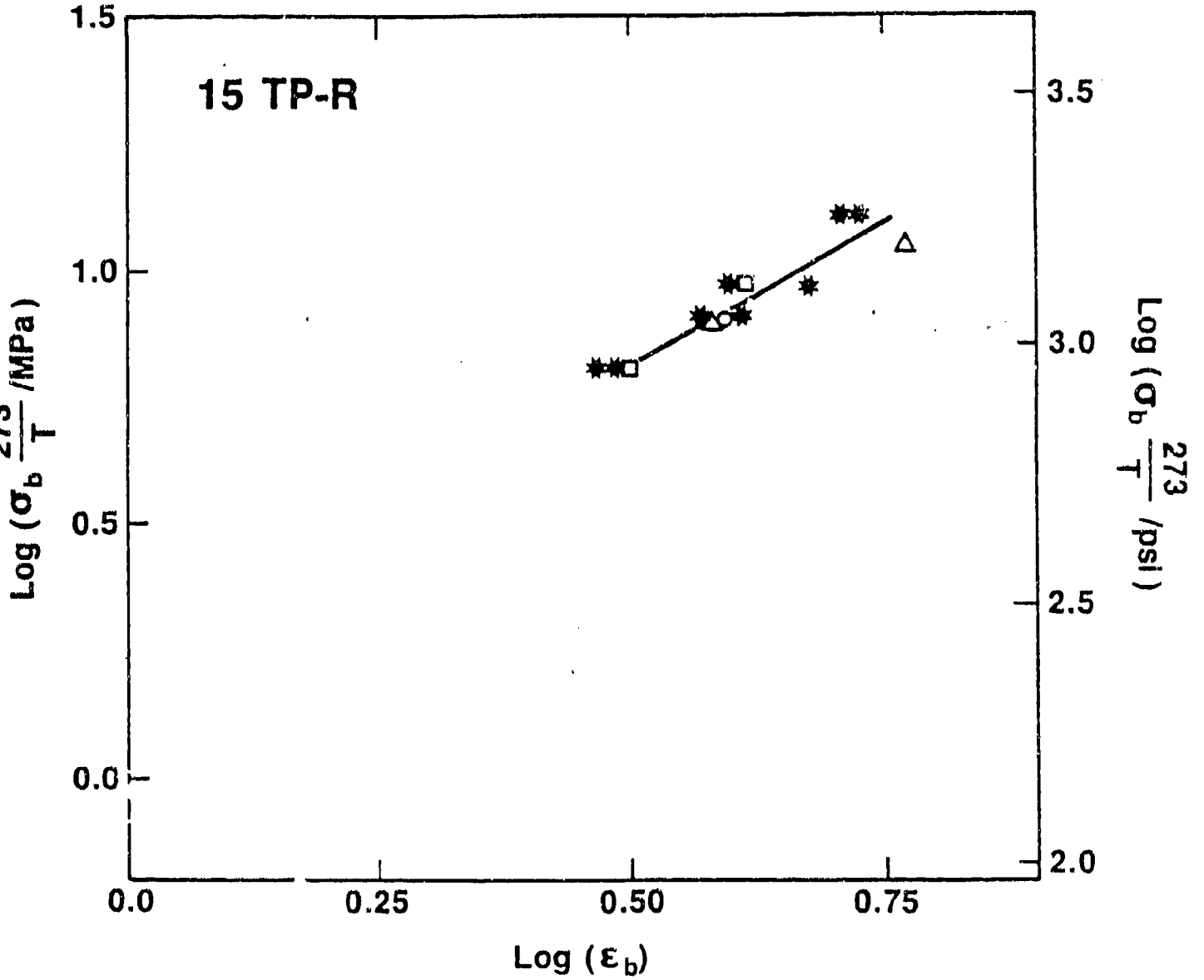

Figure 3-28 Fatigue failure envelope obtained under zero-tension sinusoidal loading conditions for 15TP-R rubber compound. Test frequency: (o) 0.0002 Hz; (□) 0.002 Hz; (Δ) 0.01 Hz; (*) 0.05 Hz, T = 23°C.

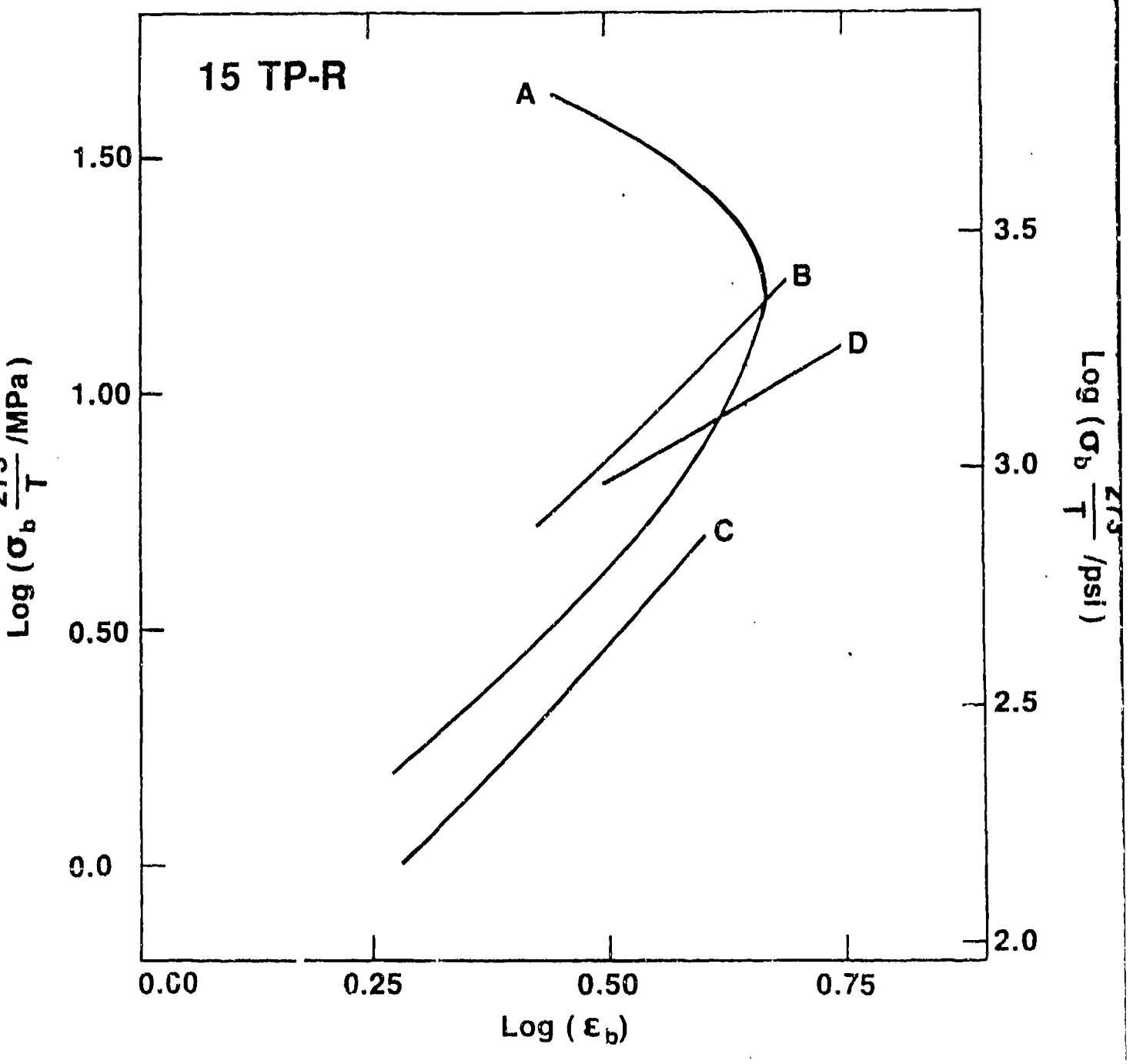

Figure 3-29 Comparison of failure envelopes for 15TP-R rubber compound obtained under different experimental conditions. (A) constant rate of deformation; (B) "low temperature" creep; (C) "high temperature" creep and (D) fatigue at 23°C.

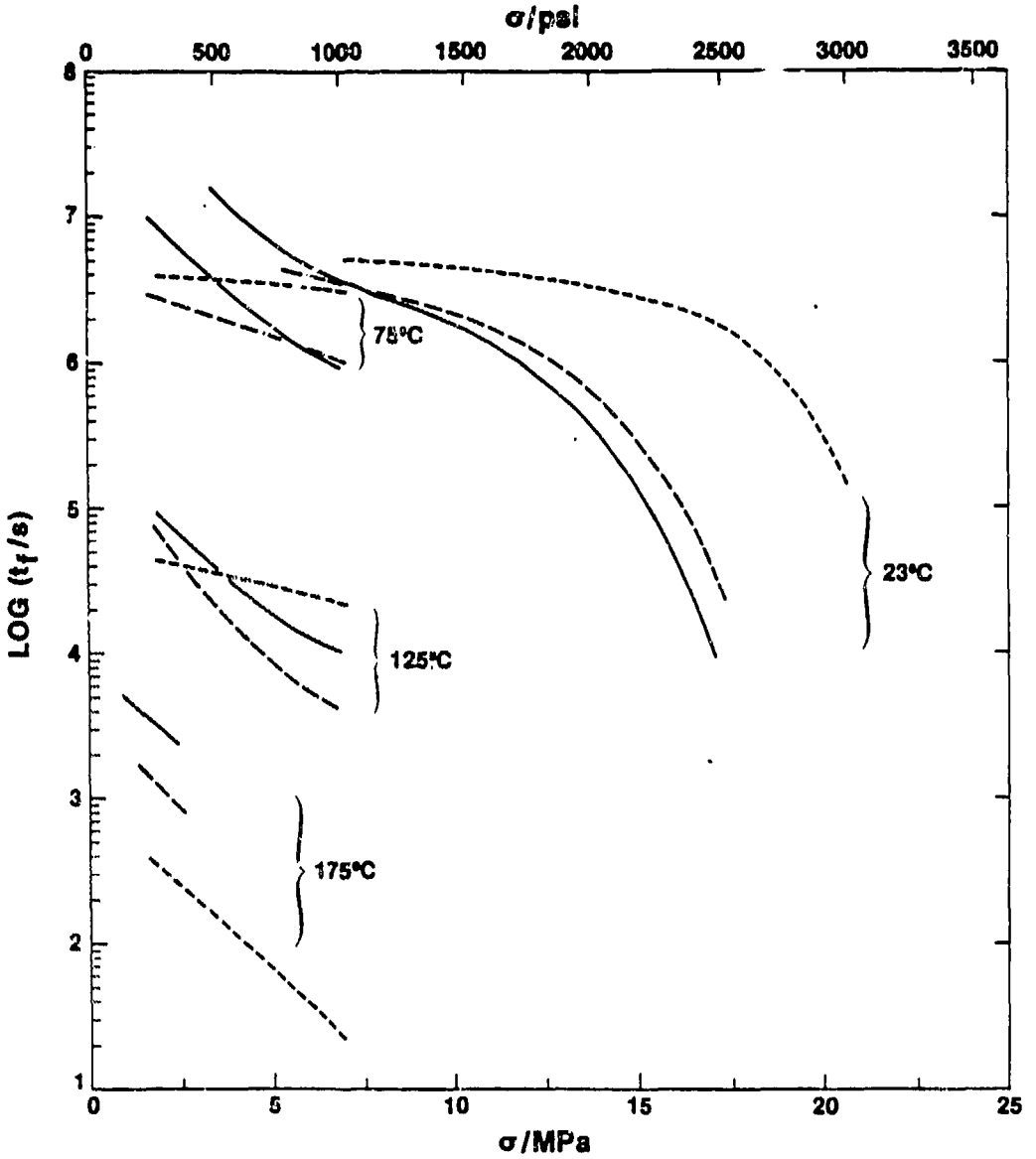

Figure 3-30 Comparison of log t_f vs. σ for TP-14AX, 15NAT-25A and 15TP-R rubber compounds at different temperatures, as indicated. Solid line: 15TP-14AX, Long Dashed Line: 15TP-R, Short Dashed Line: 15NAT-25A.

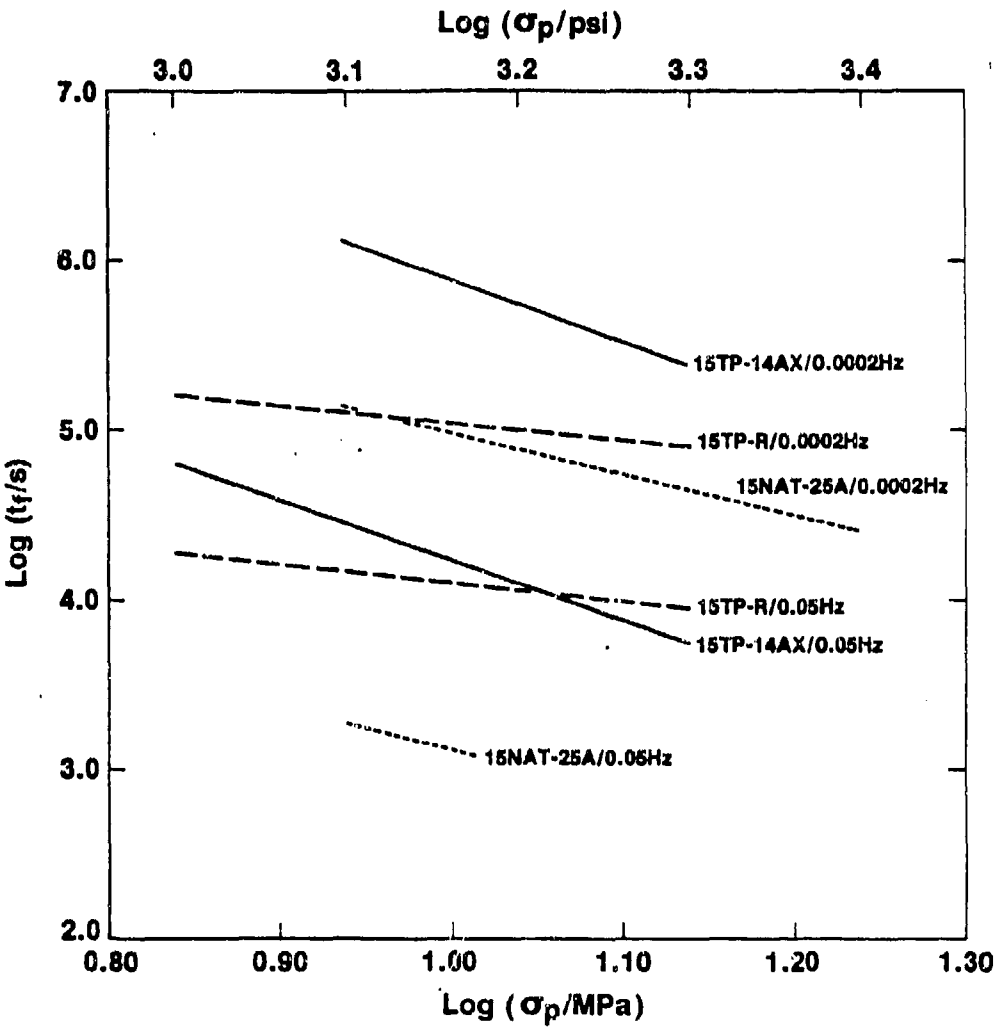

Figure 3-31 Comparison of log t_f vs log σ_p in zero-tension sinusoidal fatigure at 23°C for 15TP-14AX, 15NAT-25A and 15TP-R rubber compounds at test frequencies of 0.0002 Hz and 0.05 Hz, as indicated.